

# Persistent and Stable Radicals of the Heavier Main Group Elements and Related Species

Philip P. Power

Department of Chemistry, University of California—Davis, One Shields Avenue, Davis, California 95616

Received July 19, 2002

## Contents

I. Introduction	789
II. Group 13 Element Radicals	790
A. Boron	790
B. Aluminum, Gallium, and Indium	793
III. Group 14 Element Radicals	796
A. $\cdot\text{MR}_3$ Radicals and Related Species	796
B. Multinuclear Radicals and Radical Anions	798
IV. Group 15 Element Radicals	800
V. Radicals of the Group 16 Elements Selenium and Tellurium	804
VI. Conclusions and Outlook	805
VII. Acknowledgment	806
VIII. Note Added in Proof	806
IX. Note Added after ASAP Posting	806
X. References	806



Philip Power received his B.A. degree from Trinity College Dublin in 1974 and his D.Phil. degree, under the supervision of M. F. Lappert, from the University of Sussex in 1977. After postdoctoral studies with R. H. Holm at Stanford, he joined the faculty at the University of California, Davis, where he is currently Professor of Chemistry. His main research interests involve the structural chemistry of organoalkali metal and organocopper compounds, low-coordinate transition metal chemistry, multiple bonding in main-group chemistry, and the development of new ligands for the stabilization of low coordination number, unusual oxidation states, and multiple bonding in both transition metal and heavier main-group compounds. He is a recipient of fellowships from the A. P. Sloan and Alexander von Humboldt foundations. In addition, he has been Reilly Lecturer at the University of Notre Dame (1995), and Faculty Research Lecturer at the University of Iowa (1993) and the University of Auckland, New Zealand (1993).

## I. Introduction

The most striking difference between the chemistries of the main-group and transition elements is the ability of the latter to form stable complexes in which the oxidation states differ by unity steps. This characteristic arises from the availability of several energetically accessible, often degenerate, nonbonding or antibonding d-levels that can accommodate a variable number of unpaired electrons.<sup>1</sup> In contrast, parallel behavior in main-group species is circumscribed by several factors. First, there is a more limited number of valence orbitals available,<sup>2</sup> which are occupied to varying extents, either by bonding pairs or by nonbonding lone pairs of electrons. Stable, electron-poor, un-delocalized main-group compounds with more than one unoccupied valence level, which might accommodate unpaired electrons in a way similar to the transition metal complexes, are extremely rare. The few known examples require very large or  $\pi$ -bonding ligands for stability.<sup>3</sup> Main group species with one empty acceptor valence orbital are less rare, but they are often prone to associate either with themselves or with Lewis bases unless they are sterically protected. For later main-group element derivatives, the valence orbitals are fully occupied by lone pairs and/or bond pairs, and it becomes increasingly difficult to create odd-electron species by oxidation or reduction. This is due, on one hand, to the greater electronegative character of these elements, and on the other, to the lack of a suitable low-energy orbital to accept an electron. As a result, ionic

radicals generated from these compounds are often very reactive, owing to either their avidity for electrons or their instability due to increased interelectronic repulsion.<sup>4</sup> There are similar difficulties with radicals generated by homolytic cleavage of bonds where, with rare exception, extremely reactive fragments are formed which either decompose or react very rapidly to give diamagnetic products.

Despite these restrictions, numerous persistent or stable,<sup>5</sup> odd-electron main-group species based on the first-row elements C, N, and O are known. The molecules  $\text{O}_2$ , NO, and  $\text{NO}_2$ , all of which contain unpaired electrons, are simple examples that have been recognized for a long time. Many classes of more complex, persistent or stable radical species centered on one or more of these elements are also well-established, in some cases since the 19th century. The latter include Fremy's salt  $\text{K}_2\{\text{ON}(\text{SO}_3)_2\}$ ,<sup>6</sup> Wurster salts (singly oxidized salts of *p*-phenylenediamines),<sup>7</sup> the metal ketyl  $\text{MOCR}_2$ ,<sup>8</sup> and the Gomberg radical  $\cdot\text{CPh}_3$ .<sup>9</sup> In general, they are stabilized by a combina-

tion of electronic effects (relatively high electronegativity of the main-group atom), partial spin delocalization onto substituents, and/or steric effects.<sup>10</sup> For example, the persistence of  $\cdot\text{CPh}_3$  in solution is believed to be due to a combination of resonance and steric contributions.<sup>11</sup> In addition to the radicals of first-row elements, several persistent or stable radicals in which unpaired electron density is delocalized in part onto sulfur have been characterized. Many of them incorporate sulfur as part of an aromatic ring<sup>12,13</sup> or a sulfur–nitrogen<sup>14,15</sup> ring. The range of such compounds is relatively large and is expanding rapidly, and several have been structurally characterized.<sup>16–21</sup> The treatment of these important compounds in sufficient detail is beyond the scope of this review.

Stable radicals with an unpaired electron located primarily on main-group atoms other than those common in organic compounds, i.e., C, N, O, and S, are much less studied. Although a very large number of radical compounds of “inorganic” elements had been generated, trapped in low-temperature matrices, and studied by EPR spectroscopy,<sup>22,23</sup> it was not until the mid-1970s that the first persistent examples (i.e., derivatives of the heavier group 14<sup>24</sup> and group 15<sup>25</sup> elements) were synthesized and characterized in solution, and the early results have been summarized in a review.<sup>26</sup> Several of the radicals had half-lives of  $>1$  year, and their persistence was due primarily to steric effects. The ensuing years have seen the expansion of this work to several new radical derivatives of these elements, and the range of odd-electron species has been broadened to include several that are centered on the group 13 elements. An important development of the recent work has been the crystallization and detailed structural characterization of a diverse selection of stable radicals. In conjunction with EPR spectroscopic studies and computational work, this has allowed detailed insight into their electronic structure and bonding. The major objective of this review is to summarize the data for persistent or stable odd-electron species in which the unpaired electron is located primarily on main-group elements other than C, N, O or S and to show that, under suitable steric and electronic conditions, many such species can be obtained as stable crystalline compounds.<sup>5</sup>

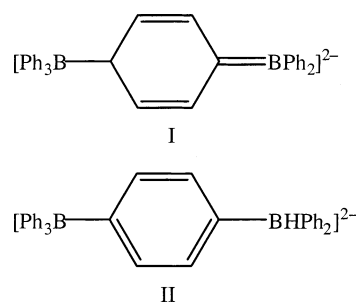
The following abbreviations will be used: Ar\*,  $-\text{C}_6\text{H}_3-2,6\text{-Trip}_2$ ; dbdab, 1,4-di-*tert*-butyl-1,4-diazabutadiene; DME, 1,2-dimethoxyethane; Dmp,  $\text{C}_6\text{H}_2-2,6\text{-Mes}_2$ ; Dxp,  $-\text{C}_6\text{H}_2-2,6(2,6\text{-Me}_2\text{C}_6\text{H}_3)_2$ ; en, 1,2-ethylenediamine; Mes, mesityl or 2,4,6-trimethylphenyl; Mes\*,  $-\text{C}_6\text{H}_2-2,4,6\text{-Bu}^t_3$ ; pz, pyrazine; TMEDA, *N,N,N,N*-tetramethylethylenediamine; Trip, 2,4,6-trisopropylphenyl; (2.2.2) = Kryptofix222, 4,7,13,16,21,-24-hexaaza-1,10-diazabicyclo[8.8.8]hexacosane.

## II. Group 13 Element Radicals

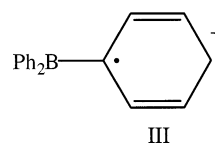
### A. Boron

Since the electron configuration of boron differs from that of carbon by just one electron, attempts to synthesize isoelectronic boron-centered analogues (i.e.,  $\text{BAR}_3^{\cdot-}$ ) of the  $\cdot\text{CAR}_3$  radicals have a relatively

long history. In 1926, Krause and co-workers showed that triphenylboron could be reduced with alkali metals in ether to give colored salts of formula  $\text{MBPh}_3$  ( $\text{M} = \text{Li}–\text{Cs}$ ).<sup>27</sup> The reduction of several other  $\text{BR}_3$  species ( $\text{R} = p\text{-tolyl}$ ,<sup>28</sup> cyclohexyl,<sup>28</sup> benzyl,<sup>29</sup> Pr,<sup>30</sup> and Bu<sup>t</sup><sup>30</sup>) was also investigated. Later work showed that the  $\text{Na}^+$  salt of  $[\text{BPh}_3]^-$  is diamagnetic in THF and in the solid state, and it was assumed that the  $\text{Na}^+[\text{BPh}_3]^-$  ion pairs were associated to form clusters.<sup>31</sup> Further experiments showed that the  $[\text{BPh}_3]^-$  could be formed in 1,2-dimethoxyethane (DME). EPR studies of  $[\text{BPh}_3]^-$ , its deuterated analogues, and  $[\text{B}(\text{C}_6\text{H}_4\text{-}4\text{-X})_3]^-$  ( $\text{X} = \text{Cl}$  or OMe) showed that the unpaired electron was located primarily at boron, with  $a(^{11}\text{B}) = 7.84$  G, and coupling to ring hydrogens was also observed.<sup>32</sup> The relatively low value of the boron hyperfine coupling indicates that the unpaired electron density is associated with the boron 2p-orbital and that the boron geometry is planar rather than pyramidal. The most recent  $^1\text{H}$  and  $^{11}\text{B}$  NMR studies<sup>33</sup> of the reduction of  $\text{BPh}_3$  in ether solution by sodium metal indicate that, as is the case with  $\text{CPh}_3$ ,<sup>34</sup> a head-to-tail dimer **I** is formed which rearranges to **II** upon heating. Prolonged reaction of  $\text{BPh}_3$



with sodium leads to various decomposition products, including biphenyl,  $\text{NaBPh}_4$ , and sodium phenylborohydrides. The formation of **I** can be explained by the initial formation of **III** and its subsequent coupling to give **I**.<sup>33</sup>



The use of bulkier aryl substituents such as mesityl,<sup>35</sup>  $\beta$ -methylnaphthyl,<sup>36</sup> and  $\alpha$ -naphthyl<sup>37</sup> afforded monosodium salts which are paramagnetic monomers in THF or  $\text{Et}_2\text{O}$  solution. EPR spectroscopy of  $[\text{BMes}_3]^-$  showed hyperfine coupling to  $^{11}\text{B}$  [ $a(^{11}\text{B}) = 9.87–10.32$  G and  $a(^1\text{H}) = 1.10–1.98$  G].<sup>38–41</sup> The value of the boron hyperfine coupling is slightly higher than that in  $[\text{BPh}_3]^-$ <sup>32,40</sup> but is fully consistent with planar boron coordination. Further interpretation of the EPR spectroscopic parameters suggested that the spin density in the  $^{11}\text{B}$  2p<sub>z</sub>-orbital is ca. 0.5,<sup>40</sup> which is similar to the value (0.65) for  $\cdot\text{CPh}_3$ .<sup>41,42</sup>

It has proven possible to crystallize the anion  $[\text{BMes}_3]^-$  as the solvent-separated ion-pair salt  $[\text{Li}(12\text{-crown-}4)_2][\text{BMes}_3]$  by the addition of 12-crown-4 to solutions of  $\text{LiBMes}_3$  in THF.<sup>43</sup> The crystals proved to be remarkably thermally stable, not decomposing

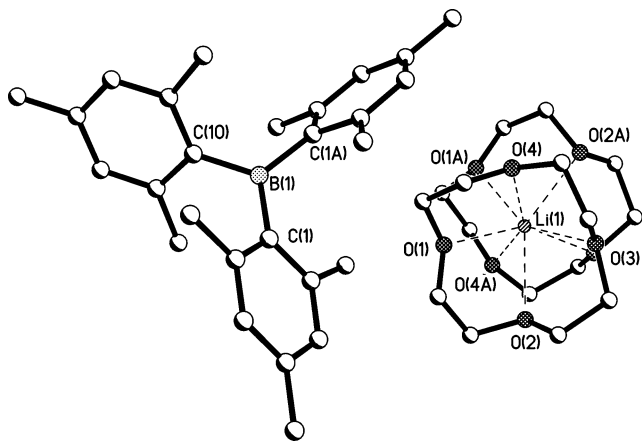
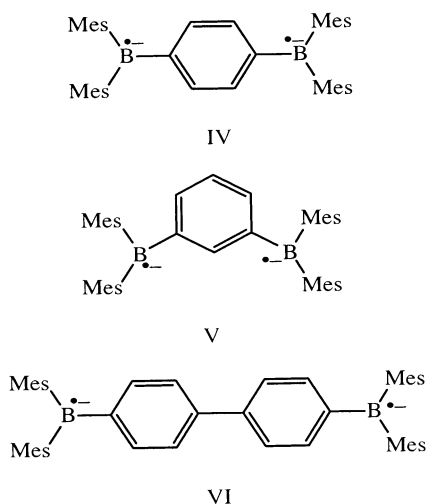


**Figure 1.** Schematic drawing of the salt  $[\text{Li}(12\text{-crown-4})]_2[\text{BMes}_3]$ .<sup>43</sup>

until ca. 240 °C in the melting point apparatus. The structure (Figure 1) showed that the cations and anions are well-separated. The coordination at boron is planar, with only slight deviation in the C–B–C angles from 120°. There is a slight lengthening (ca. 0.02 Å) in the B–C bonds in comparison to the bonds in the neutral precursor  $\text{BMes}_3$ . The dihedral angles between the mesityl planes and that at boron are very similar in the reduced and unreduced species. These stable triaryl boron radicals have also been studied electrochemically, and the most recent results have involved derivatives in which one or more of the aryl rings is coordinated by a transition metal carbonyl fragment.<sup>44</sup> In addition, the triplet diradical dianions **IV**,<sup>45</sup> **V**,<sup>46</sup> and **VI**<sup>47</sup> could be obtained at room temperature via reduction of the corresponding neutral compound electrochemically (**IV**) or with sodium (**V**). It was pointed out that **IV** and related phenyl



and 9-borabicyclo[3.3.1]nonyl derivatives are mirror images of the corresponding cationic *p*-phenylenediamine. They display two reversible reduction peaks, but their EPR spectra have no hyperfine structure because of the large number of couplings from substituent hydrogens. Recent studies have also shown that the halogenated species  $[\text{B}(\text{C}_6\text{F}_5)_3]^{2-}$  can be generated. However, it is significantly less stable than the sterically crowded triarylboron anions and it has a  $t_{1/2}$  of ca. 2 min at room temperature.<sup>48</sup>

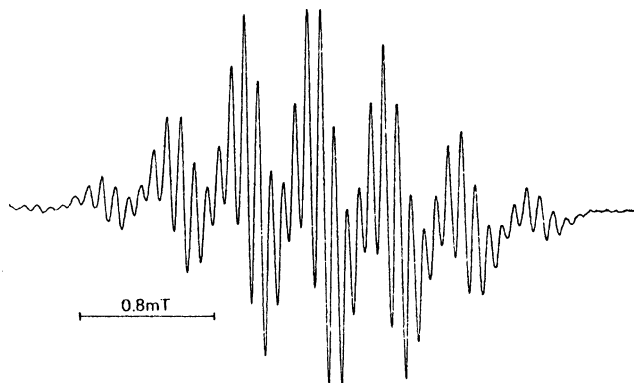
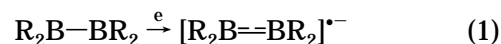


**Figure 2.** Illustration of the EPR spectrum of  $[\{\text{CD}_3\}_3\text{-CCH}_2\}_2\text{BB}\{\text{CH}_2\text{C}(\text{CD}_3)_3\}_2]^{2-}$  in DME at 30 °C.<sup>54</sup>

Persistent trialkylboron  $[\text{BR}_3]^{2-}$  radicals could also be obtained by use of bulky substituents such as  $\text{Bu}^t$  or  $-\text{CH}_2(\text{Bu}^t)$ . The  $a(^{11}\text{B})$  hyperfine coupling of  $[\text{B}\{\text{CH}_2(\text{Bu}^t)\}_3]^{2-}$  is 28 G, while that of  $[\text{B}(\text{Bu}^t)_3]^{2-}$  is 38.5 G.<sup>49</sup> These values are significantly higher than those cited above for the triaryl radicals, indicating increased spin density at boron. Replacement of one of the alkyl groups by a  $-\text{CH}=\text{CH}(\text{Bu}^t)$  or a  $-\text{C}_6\text{H}_3\text{-3,5-Bu}^t_2$  substituent dramatically lowers the  $^{11}\text{B}$  couplings to 8.4 and 9.3 G, respectively. It was concluded that the lower coupling values for the aryl and alkenyl derivatives are due to increased delocalization of spin in these complexes.

The synthesis of the first stable tetraalkyldiboron(4) compounds in 1980<sup>50,51</sup> paved the way for reduction of adjacent boron centers containing empty *p*-orbitals.<sup>52,53</sup> One-electron reduction of such compounds in solution in accordance with eq 1 afforded the persistent radical  $[\text{R}_2\text{B}=\text{BR}_2]^{2-}$ , in which there is a one-electron B–B  $\pi$ -bond. EPR spectroscopy of



the  $\text{Bu}^t$ -substituted species displayed coupling constants of  $a(^{11}\text{B}) = 14.4$  G (2B) and  $a(^1\text{H}) = 5.4$  G. The boron coupling is similar to the values noted earlier for  $[\text{BPh}_3]^{2-}$  and  $[\text{BMes}_3]^{2-}$ . The coupling results in a 1:2:3:4:3:2:1 septet pattern that is characteristic for interaction of the unpaired electron with two equivalent  $^{11}\text{B}$  nuclei. The neopentyl-substituted radical displayed equivalent coupling to two borons, with  $a(^{11}\text{B}) = 0.8$  G, and  $a(^1\text{H})$  coupling of 3.8 and 4.65 G to two equivalent sets of four  $\alpha$ -hydrogens (Figure 2).<sup>54</sup> The assignment of the larger coupling to the hydrogens was verified by D atom substitution. The nonequivalence of the methylene hydrogen couplings indicated that the neopentyl groups adopt a preferred conformation in which diagonally opposed  $\text{Bu}^t$  groups occupy alternating positions above and below the molecular plane, thus accounting for inequivalent  $\alpha$ -hydrogen positions. Another feature of interest is that the radical is more stable ( $t_{1/2} =$  ca. 15 min, 140 °C) than its neutral precursor ( $t_{1/2} =$  ca. 20 min, 20 °C). Attempts to doubly reduce the tetraalkyldiboron(4) species were unsuccessful. The reduction of the diborane(4)  $\text{R}(\text{Cl})\text{BB}(\text{Cl})\text{R}$  [ $\text{R} = \text{C}(\text{CH}_3)_3$  or  $\text{C}(\text{CD}_3)_3$ ] afforded the tetraboron(4) radical anion  $[\text{B}_4\text{R}_4]^{2-}$  as well as  $\text{B}_4\text{R}_4$ .<sup>55</sup> The EPR spectrum (Figure 2) of the

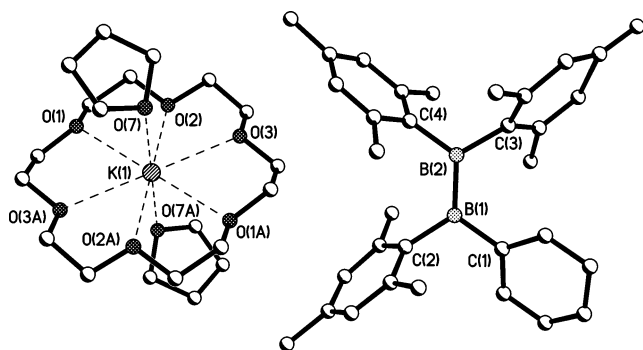
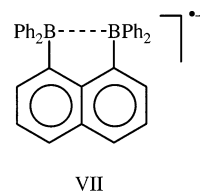


**Figure 3.** Schematic drawing of the salt  $[K(18\text{-crown-6})\text{-(THF)}_2][\text{Mes}_2\text{BB(Ph)Mes}]$ .<sup>60</sup>

perdeuterated anion has a 13-line pattern consistent with coupling to four  $^{11}\text{B}$  nuclei. A puckered cyclo-tetraborane structure has been proposed on the basis of these spectra.

The use of aryl substituents at the borons greatly enhances the stability of the neutral diborane(4) precursors. More importantly, it was possible to doubly reduce the aryl-substituted compounds and related derivatives to give  $[>\text{B}=\text{B}<]^{2-}$  ions with a formal B–B double bond.<sup>56–58</sup> In addition, singly reduced species in which the formal B–B bond order is 1.5 could also be isolated for the first time.<sup>59,60</sup> They were crystallized by using a stoichiometric amount of reducing agent. This enabled the first structural characterization of a stable diborane(4) radical in the form of the contact ion pair  $\{\text{Li}(\text{Et}_2\text{O})_2\}\text{MeO}(\text{Mes})\text{-BB}(\text{Mes})\text{OMe}$ , which was obtained as dark blue crystals.<sup>59</sup> Unfortunately, no hyperfine coupling could be seen in the broad EPR signal due to this species. However, the X-ray crystal structure showed that  $\text{Li}^+$  is bound to the monoanion by coordination to the methoxy oxygens. The B–B bond length is 1.636(7) Å, which is ca. 0.09 Å shorter than the 1.724(9) Å bond length in the neutral precursor, in agreement with the formation of a B–B  $\pi$ -bond of order 0.5. This distance resembled those observed in the doubly reduced  $\{\text{Li}(\text{Et}_2\text{O})_2\}_2\{\text{Mes}_2\text{BB(Ph)Mes}\}$  [ $\text{B}=\text{B} = 1.636\text{-(11) Å}$ ]<sup>56</sup> and  $\{\text{Li}(\text{Et}_2\text{O})_2\}_2\{(\text{Me}_2\text{N})\text{PhBBPh}(\text{NMe}_2)\}$  [ $\text{B}=\text{B} = 1.627(9) \text{ Å}$ ].<sup>58</sup> It is thought that the increased Coulombic repulsion produced by the addition of the second electron roughly equals the shortening expected from the increase in formal bond order from 1.5 to 2. A further example of a structurally characterized diborane(4) radical anion resulted from the one-electron reduction of  $\text{Mes}_2\text{BB(Ph)Mes}$  by potassium in THF.<sup>60</sup> This afforded, upon adding 18-crown-6, the solvent-separated ion pair  $[K(18\text{-crown-6})\text{-(THF)}_2][\text{Mes}_2\text{BB(Ph)Mes}]$  as dark purple crystals. The structure (Figure 3) displayed an average B–B bond length of 1.649(11) Å and a small torsion angle between the boron coordination planes of 6.9°, in comparison to the 1.706(12) Å and 79.1° in the neutral  $\text{Mes}_2\text{BB(Ph)Mes}$ . These parameters and others in the structure are consistent with a  $\pi$ -bond of order 0.5. The EPR spectrum in THF solution at 25 °C displayed hyperfine coupling to the  $^{11}\text{B}$ – $^{11}\text{B}$  isotopomer which gave a seven-line pattern with  $a(^{11}\text{B}) = 13 \text{ G}$ , which was similar to the value observed for the tetraalkyl anions and consistent with the formation of the  $\pi$ -radical.

A different type of radical was obtained by reduction of 1,8-bis(diphenylboryl)naphthalene by potassium in THF/18-crown-6, which resulted in a paramagnetic purple solution consistent with the formation of the  $\sigma$ -radical VII, which is stable for several weeks at  $-25 \text{ °C}$ .<sup>61</sup> The EPR spectrum displayed hyperfine



coupling to two borons, with  $a(^{11}\text{B}) = 5.9 \text{ G}$ , consistent with the formation of a one-electron  $\sigma$ -bond. Unfortunately, no X-ray crystal data have been obtained, but DFT calculations indicated a B–B bond length of 2.82 Å, which is ca. 0.2 Å shorter than the B–B distance in the neutral precursor.

The formation of polyhedral boron cage radicals has been known since the 1960s.<sup>62</sup> They were obtained via either oxidation or reduction reactions. The oxidation of  $\text{K}_2\text{B}_{10}\text{H}_{10}$  by  $\text{CuCl}_2$  or  $\text{FeCl}_3$  produced the radical  $[\text{B}_{10}\text{H}_{10}]^{\cdot-}$  in solution which was stable enough for EPR and UV–vis data to be obtained at room temperature. In addition,  $[\text{B}_8\text{H}_8]^{\cdot-}$  was identified as one of the transient products from the oxidation of  $[\text{B}_9\text{H}_9]^{2-}$ , with  $a(^{11}\text{B}) = 2.52 \text{ G}$  and  $a(^{10}\text{B}) = 0.84 \text{ G}$ . Later, it was discovered that, upon oxidation, the perhalogenated borane clusters afforded radical anions that were much more stable. The first of these were the  $[\text{B}_9\text{X}_9]^{\cdot-}$  ( $\text{X} = \text{Cl}, \text{Br}, \text{or I}$ ) species, which displayed broad EPR signals in solution and were indefinitely stable under anaerobic and anhydrous conditions at room temperature.<sup>63a</sup> In addition, reversible interconversion between the three oxidation states,  $[\text{B}_9\text{X}_9]^{0/1-/2-}$ , was established. Recently, an improved synthesis of the  $\text{B}_9\text{X}_9$  ( $\text{X} = \text{Cl}, \text{Br}, \text{or I}$ ) series and the reduction of these species to the anions  $[\text{B}_9\text{X}_9]^{\cdot-}$  and  $[\text{B}_9\text{X}_9]^{2-}$  have been reported.<sup>63b</sup> The paramagnetic radical anions were characterized by magnetic susceptibility measurements of  $[\text{Cp}_2\text{M}][\text{B}_9\text{X}_9]$  ( $\text{M} = \text{Fe or Co}$ ). Their EPR spectra in frozen  $\text{CH}_2\text{Cl}_2$  displayed increasing  $g$ -anisotropy for the heavier halogen derivatives, indicating significant halogen participation in the singly occupied MO.<sup>63b</sup> Detailed investigations of the series  $[\text{B}_6\text{X}_n\text{H}_{6-n}]^{2-}$  ( $\text{X} = \text{Cl}, \text{Br}, \text{I}; n = 1\text{--}6$ ) showed that redox reactions were reversible only for the halides and  $\text{trans-}[\text{B}_6\text{-Br}_4\text{H}_2]^{2-}$ .<sup>64</sup> The deep blue  $[\text{B}_6\text{I}_6]^{\cdot-}$ , orange  $[\text{B}_6\text{Br}_6]^{\cdot-}$ , and yellow-green  $[\text{B}_6\text{Cl}_6]^{\cdot-}$  radical anions were characterized by electronic, IR/Raman, and magnetic measurements. The crystal structures of the salts  $[\text{NBu}^n_4][\text{B}_6\text{X}_6]$  and  $[\text{N}(\text{PPh}_3)_2][\text{B}_6\text{I}_6]$  were also determined.<sup>64</sup> The gross structural distortions originally reported for the  $\text{B}_6$  cage in  $[\text{NBu}^n_4][\text{B}_6\text{I}_6]$ <sup>64a</sup> were not observed in  $[\text{NBu}^n_4][\text{B}_6\text{X}_6]$  ( $\text{X} = \text{Cl or Br}$ ) or in  $[\text{N}(\text{PPh}_3)_2][\text{B}_6\text{I}_6]$ <sup>64b</sup> (Figure 4), where average B–B distances near 1.73 Å and angles near idealized values were observed within the  $\text{B}_6$  octahedron. These parameters may be compared with those in the corresponding dianions, where B–B distances in the

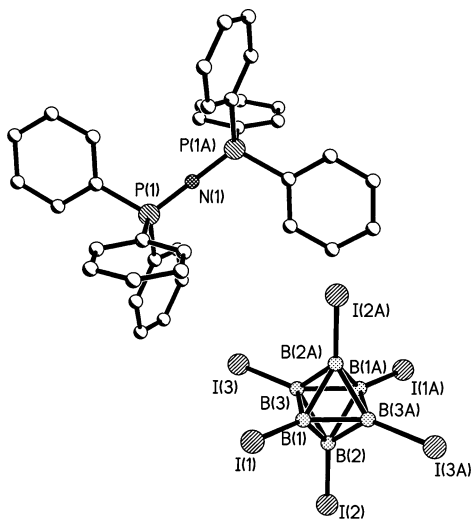
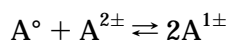


**Figure 4.** Schematic drawing of the salt  $[N(PPh_3)_2][B_6I_6]$ .<sup>64b</sup>

range 1.64(2)–1.67(2) Å and cage angles within 1° of the idealized values for  $O_h$  symmetry were observed. More recent EPR studies showed that the iodine species displayed considerable  $g$ -anisotropy and rapid relaxation, so spectra could be observed only at low temperatures.<sup>65</sup> No hyperfine interactions were evident, due possibly to the low resolution as a result of many overlapping lines, or to relatively small coupling. The latter explanation seems likely, since a study of  $[^{11}B_6Cl_6]^{2-}$  (99.5°/<sup>11</sup>B) showed that it displayed no difference in EPR signals from the cluster which had naturally occurring isotopic abundances. Further work on a variety of radical clusters resulted in the characterization of  $[BX_nX'_{6-n}]^{\cdot-}$ ,  $[B_6X_5R]^-$  (X or X' = Cl, Br, or I; R = CH<sub>2</sub>CN, CH<sub>3</sub>, or H) by cyclic voltammetry, EPR, vibrational, and UV-vis spectroscopy.<sup>66</sup> The EPR data displayed increasing  $g$ -anisotropy and EPR line widths in the sequence Cl < Br < I. The substitution of just one halide by –CH<sub>2</sub>CN, CH<sub>3</sub>, or I caused greatly decreased radical persistence. Parallel studies on the chemistry of  $B_nCl_n^{0/1-2-}$  ( $n = 8$  or 9) by cyclic voltammetry and EPR spectroscopy showed that the hyperdeficient boron subhalide clusters readily underwent reduction by trace amounts of moisture that is usually present even in dried solvents, so the starting material in the voltametric experiment starts from the ions  $B_nCl_n^{\cdot-}$  ( $n = 8$  or 9), which can undergo quasi-reversible reduction to the dianion or oxidation to the neutral species.<sup>67</sup> Calculation of equilibrium constants for the disproportionation reaction

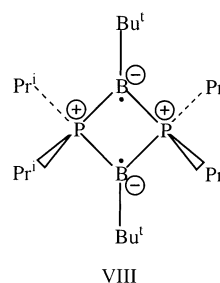


gave values for  $K$  of about  $10^9$ , showing that the monoanion is stable to disproportionation.

The icosahedral carborane  $\cdot CB_{11}Me_{12}$  was the first isolated, neutral boron cluster radical.<sup>68</sup> It was prepared by the oxidation of  $Cs^+[CB_{11}Me_{12}]^-$  either with  $PbO_2/CF_3COOH$  or by electrochemical techniques. It exists as black crystals that are stable in air for a few days and soluble in hydrocarbon or ether solvents. The EPR spectrum in solution or in low-temperature glasses displayed a broad absorption

(peak-to-peak width = 37 G) with no hyperfine structure. The stability of the radical was attributed to the delocalization and steric protection by the sheath of methyl groups,<sup>68</sup> although calculations indicated a high ionization potential of 4.32 eV for the corresponding anion,  $CB_{11}Me_{12}^-$ .<sup>69</sup> The average lengths of the 30 edge and the 12 cage carbon bonds are 0.03 and 0.02 Å longer than those in the anion. This is in keeping with the lower cage bond order in the neutral species.<sup>70</sup> More recent work has shown that one-electron oxidation of the *closo*- $[B_{12}Me_{12}]^{2-}$  dianion by  $Ce^{4+}$  affords the radical anion salt  $[N(PPh_3)_2][B_{12}Me_{12}]$ . Remarkably, this species is air stable and may be reconverted to the dianion by reduction with  $NaBH_4$ .<sup>70</sup>

A very recent development in the area of boron radical chemistry has been the isolation of the unusual compound **VIII**, in which electrons of op-



**VIII**

posite spin are located on each boron.<sup>71</sup> The compound was prepared in 68% yield and has a melting point of 212 °C. The important features of the molecule are that it is EPR silent between –80 °C and room temperature and has a long B–B separation of 2.57 Å (cf. ca. 1.7 Å for a B–B single bond and 2.82 Å for the one-electron B–B  $\sigma$ -bond in **VII**<sup>61</sup>). The <sup>11</sup>B and <sup>31</sup>P NMR signals appear within the expected ranges. Calculations showed that the triplet state lies 17.2 kcal mol<sup>–1</sup> above the singlet state, which suggests significant coupling between the borons. A plot of the HOMO of this compound indicated the presence of a weak  $\pi$ -interaction between the boron centers. Another class of boron radicals are derivatives of diborene, HBBH. Spectroscopic<sup>72</sup> and theoretical<sup>73</sup> data indicated that HBBH exists as a linear triplet, but no derivatives have been stabilized so far.

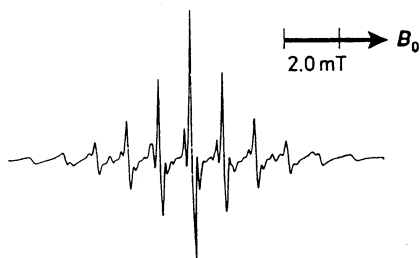
## B. Aluminum, Gallium, and Indium

Stable radicals having an unpaired electron located primarily on a heavier group 13 element have only been known since 1993.<sup>74</sup> Prior to that date, several stable radicals containing the elements Al, Ga, or In, in which the spin was delocalized over an unsaturated, usually cyclic, organic substituent array, were known. These include *i*-Bu<sub>2</sub>Al·2,2'-bipyridyl, [4,4'-bipyridyl]{AlR<sub>2</sub>(THF)}<sub>2</sub><sup>•+</sup> or pyrazine derivatives [pz(MR<sub>2</sub>)<sub>2</sub>]<sup>•+</sup>[MR<sub>4</sub>]<sup>–</sup> (R = Me and M = Al, Ga, In; R = Et and M = B, Al),<sup>75–78</sup> the tris-1,3-diphenyltriazenido (dpt) complexes M(dpt)<sub>3</sub> (M = Al, Ga, or In),<sup>79</sup> or the 1,4-di-*tert*-butyl-1,4-diazabutadiene (dbdab) complex Al(dbdab)<sub>2</sub> as well as its gallium analogue.<sup>80–82</sup> However, EPR studies showed that the latter radicals should be formulated as (dbdab<sup>–</sup>)M-

**Table 1. Metal–Metal Bond Lengths and Torsion Angles Illustrating the Structural Differences between the Neutral Compounds  $R_2MMR_2$  and Their Singly Reduced Radical Analogues  $[R_2MMR_2]^-$  ( $M = Al$  or  $Ga$ ;  $R = Alkyl$  or  $Aryl$ )**

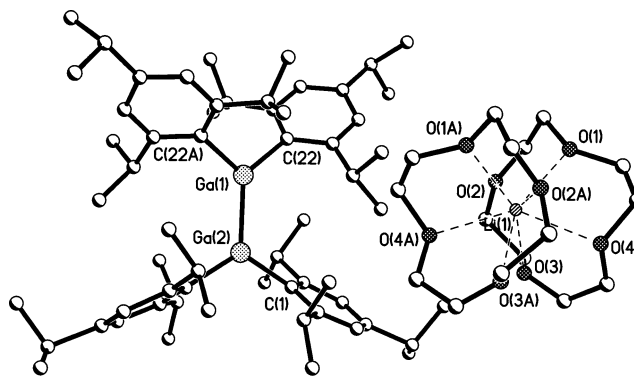
	M–M (Å)	torsion angle (deg) <sup>a</sup>	M–C (Å)	refs
$R_2AlAlR_2$ [ $R = CH(SiMe_3)_2$ ]	2.660(1)	4.3	1.982(3)	85
$R'_2AlAlR'_2$ [ $R' = C_6H_2-2,4,6-Pr^i_3$ ]	2.647(3)	44.8	1.996(3)	88
$[R_2AlAlR_2]^-$	2.53(1)	0	2.040(5)	74a
$[R'_2AlAlR'_2]^-$	2.470(2)	1.4	2.021(1)	88
$R_2GaGaR_2$ [ $R = CH(SiMe_3)_2$ ]	2.541(1)	8.0	1.995(5)	86
$R'_2GaGaR'_2$ [ $R' = C_6H_2-2,4,6-Pr^i_3$ ]	2.515(3)	43.8	2.008(7)	74b
$[R_2GaGaR_2]^-$	2.401(1)	0	2.064(5)	89
$[R'_2GaGaR'_2]^-$	2.343(2)	15.5	2.038(10)	74b

<sup>a</sup> Angle between metal coordination planes.

**Figure 5.** Illustration of the EPR spectrum of  $[(Me_3Si)_2CH]_2AlAl[CH(SiMe_3)_2]_2^-$  in THF at 60 °C.<sup>72</sup>

(dbdab)<sup>2-</sup>, i.e., M(III) derivatives in which the spin is located on the dbdab ligand.<sup>83a</sup> Radical compounds of aluminum were reviewed in 1993.<sup>84</sup>

The already discussed reduction of the diborane-(4) species to give mono-<sup>53,54,59,60</sup> or dianions<sup>56–58</sup> suggested that similar reactions should be possible for the heavier element tetraorganodimetalane(4) congeners. Although Ga–Ga or In–In bonded compounds had been known for a long time, tetraorganodimetalane(4) species suitable for reduction did not become available until the late 1980s.<sup>85–87</sup> In 1993, it was shown that both tetraalkyl<sup>72,74</sup> and tetraaryl<sup>73</sup> dimetalane(4) complexes could be singly reduced to give tetraorganodialane(4) or digallane-(4) monoanions by reduction with alkali metals. The first two structurally characterized examples were  $[Li(TMEDA)_2]^+[R_2AlAlR_2]^-$  [ $R = -CH(SiMe_3)_2$ ]<sup>74a</sup> and  $[Li(12-crown-4)_2]^+[R'_2GaGaR'_2]^-$  ( $R' = C_6H_2-2,4,6-Pr^i_3$ ).<sup>74b</sup> Key structural details for the four currently known salts of this type are given in Table 1.<sup>74,85–89</sup> The addition of one electron caused bond shortening in the range 0.13–0.18 Å (ca. 7–8%), which is accompanied by a decrease in the torsion angle between the metal coordination planes for the aryl species. EPR solution spectroscopy of the aluminum species (Figure 5) shows that the unpaired electron displays a pattern that indicated equal coupling to the two <sup>27</sup>Al ( $I = 5/2$ , 100%) nuclei, with  $a(^{27}Al) = 11.9$  (2Al, tetraalkyl) and 10.4 G (2Al, tetraaryl).<sup>72</sup> For the tetraalkyl anion, each of the 11 signals was flanked by <sup>29</sup>Si ( $I = 1/2$ , 4.67%) sidebands with a coupling of 4 G.<sup>74a,89</sup> Coupling to the four  $\alpha$ -CH hydrogens was not observed since, for steric reasons, these hydrogens lie in the nodal plane of the singly occupied  $\pi$ -molecular orbital. The EPR spectra of the gallium ions<sup>67,83</sup> are more complicated, since there are two gallium isotopes, <sup>69</sup>Ga ( $I = 3/2$ , 60.11%) and <sup>71</sup>Ga ( $I = 3/2$ , 39.89%). This results in the superposition of

**Figure 6.** Schematic drawing of the structure of  $[Li(12-crown-4)_2][Trip_2GaGaTrip_2]$  (Trip =  $C_6H_3-2,4,6-Pr^i_3$ ).<sup>73</sup>

three spectra due to the three possible isotopomeric pairs. The EPR spectrum of the tetraaryldigallium anion showed couplings of 35.4 (<sup>69</sup>Ga) and 43.9 (<sup>71</sup>Ga) G, consistent with the almost planar structure (Figure 6).<sup>74b</sup> The tetraalkyl digallium anion displayed couplings of  $a(^{69}Ga) = 57.4$  G and  $a(^{71}Ga) = 72.8$  G in addition to further hyperfine structure due to the silicon  $a(^{29}Si) = 5.3$  G.<sup>89</sup> The coupling constants and their temperature dependence suggested a shallow energy minimum for the planar structure, implying that the  $\pi$ -bonds are weak.

Calculations for the model species  $H_2MMH_2$ ,  $[H_2MMH_2]^{+}$ , and  $[H_2MMH_2]^{2-}$  showed that the addition of one electron is exothermic.<sup>90</sup> The planar ( $D_{2h}$ ) form of the monoanion is more stable than the twisted (by 90°)  $D_{2d}$  form by 22.7 (B), 14.8 (Al), 16.5 (Ga), and 13.4 (In) kcal mol<sup>-1</sup>, suggesting the formation of  $\pi$ -bonds of these approximate strengths. The calculations for the aluminum and gallium species are in good agreement with values inferred from  $\pi$ - $\pi^*$  transitions in  $[R'_2MMR'_2]^-$ , for which one-electron  $\pi$ -bond energies of ca. 19 (Al) and 17 (Ga) kcal mol<sup>-1</sup> were estimated.<sup>91</sup> In addition, calculations on  $[Ph_2MMPPh_2]^{2-}$  ( $M = B$  or  $Al$ ;  $n = 0, 1$ , or  $2$ ) show that the added electrons occupy a  $\pi$ -orbital.<sup>92</sup> It had been suggested that the second electron might have entered a  $\sigma^*$ - instead of a  $\pi$ -level, thereby causing decomposition by weakening the MM bond.<sup>91</sup> However, this is not the case, at least in theory, and the difficulty in forming the dianion may be due to other effects (vide infra). The calculated Al–Al distances and torsion angles in  $[Ph_2AlAlPh_2]^{0,1-,2-}$  are 2.614 Å and 85.1; 2.478 Å and 6.3°; and 2.443 Å and 3.5°.<sup>92</sup> The first two values are in good agreement with those

experimentally measured for  $R'_2AlAIR'_2$  and  $[R'_2AlAIR'_2]^-$ .<sup>88</sup>

In contrast to the results found for boron analogues, attempts to doubly reduce the tetraorganodimetalanes did not lead to  $[R_2MMR_2]^{2-}$  or  $[R'_2MMR'_2]^{2-}$ . Instead, reduction of  $[R_2AlAIR_2]^-$  in 1,2-dimethoxyethane gave ether cleavage products without Al–Al bonds.<sup>93,94</sup> The attempted double reduction of  $R'_2GaGaR'_2$  in  $NEt_3$  gave the rearranged species  $Na_2\{Ga(GaR'_2)_3\}$ , in which the central gallium is coordinated by three  $-GaR'_2$  units and the sodiums are complexed by aryl rings.<sup>95</sup> The 2- charge of the hypothetical dianion  $[Ga(GaR_2)_3]^{2-}$  is accommodated in an orbital of  $a_1$  symmetry, delocalized over the four galliums to afford shortened Ga–Ga distances near 2.39 Å and a formal Ga–Ga bond order of 1.33.

Like their boron counterparts, radical clusters of aluminum, gallium, and indium can be synthesized in solution, and some have been isolated as crystalline species. The radical anion  $[Al_6Bu'_6]^-$  was obtained by the reduction of  $Al_6Bu'_6$  with Na/K alloy in diethyl ether.<sup>96</sup> The EPR spectrum of  $[Al_6Bu'_6]^-$  in  $C_6D_6$  at room temperature afforded a 31-line hyperfine splitting pattern consistent with coupling to six equivalent aluminum nuclei [ $a(^{27}Al) = 8.2$  G]. Calculations indicated that the  $t_{2g}$  HOMO is occupied by five electrons, and so a Jahn–Teller distortion was predicted to afford  $a_{1g}$  and  $e_g$  orbitals. Cyclic voltammetric data for  $M_4R_4$  [ $M = Ga$  or  $In$ ;  $R = C(SiMe_3)_3$ ] in THF displayed a quasi-reversible reduction wave at  $-1.98$  and  $-1.99$  V with respect to ferricinium/ferrocene.<sup>97</sup> The EPR spectrum of the radical  $[Ga_4R_4]^-$  in THF at 280 K could be interpreted in terms of coupling to four equivalent galliums with  $a(^{69}Ga) = 19.3$  G and  $a(^{71}Ga) = 24.51$  G. However, the EPR signal of  $[In_4R_4]^-$  could not be detected. It was pointed out that both  $^{113}In$  (4.7%;  $I = 9/2$ ) and  $^{115}In$  (95.3%;  $I = 9/2$ ) have large spins which would result in 37 theoretical hyperfine lines spaced at more than 30 G and thus a spectral width exceeding 1100 G. Furthermore, there could be extreme EPR line-broadening due to rapid relaxation caused by the presence of close-lying excited states as well as spin-orbit coupling contributions.

Although the preparation and characterization of large clusters of group 13 metals stands as one of the major synthetic achievements of main-group chemistry,<sup>98</sup> it is not widely recognized that some of these clusters are paramagnetic. The isolation and structural characterization of the large clusters of these elements, including the radical clusters, have been reviewed recently,<sup>98,99</sup> and the bonding of these clusters has been considered in detail,<sup>98–100</sup> so only a brief description is given here. The best known example is the remarkable  $[Li_4I_2(Et_2O)_{10}][Al_{77}\{N(SiMe_3)_2\}_{20}]$  salt,<sup>101</sup> whose anion consists of a central aluminum surrounded by shells of 12, 44, and 20 aluminums, the latter shell being substituted by 20  $-N(SiMe_3)_2$  groups. Fifty-seven of the 77 aluminum atoms are “metalloid”, in that they are bound only to other aluminums. The presence of the unpaired electron was established by magnetic measurements and EPR spectroscopy. The latter displayed a broad signal even at 77 K. The large number of aluminum atoms ( $I = 5/2$ , 100%) probably make hyperfine features difficult to observe. Another ex-

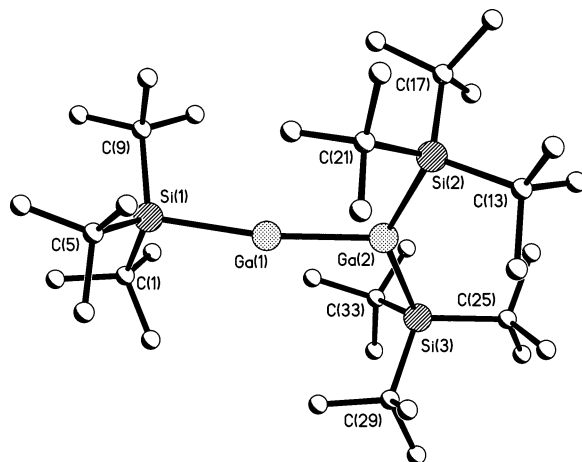


**Figure 7.** Schematic drawing of the structure of the  $R^*GaGaR_2^*$  ( $R^* = SiBu'_3$ ) radical.<sup>103</sup>

ample of a paramagnetic cluster is the salt  $[Li(Et_2O)_3][Al_{12}\{N(SiMe_3)_2\}_8]$ .<sup>102</sup> The unpaired electron was detectable by EPR spectroscopy, but no hyperfine coupling was apparent. The structure consists of an elongated framework of aluminum atoms with triangular faces in which 8 of the 12 aluminum atoms carry  $N(SiMe_3)_2$  substituents. In this case, none of the aluminums is “metalloid”.

The compounds  $R^*MMR_2^*$  ( $M = Al$  or  $Ga$ ;  $R^* = -SiBu'_3$ )<sup>103–105</sup> are the simplest stable neutral radical compounds of aluminum or gallium. They were synthesized by the reaction of excess  $NaSiBu'_3$  with  $MCl_3$ . The gallium compound<sup>103,105</sup> (Figure 7) has been structurally characterized. It has a Ga–Ga bond length of 2.423(1) Å and a wide  $[170.45(6)^\circ]$   $Si(1)-Ga(1)-Ga(2)$  angle. The M–M bonding involves overlap of  $sp(Ga(1))$  and  $sp^2(Ga(2))$  hybridized metals to afford a Ga–Ga  $\sigma$ -bond. A bonding  $\pi$ -molecular orbital is formed by overlap of two metal  $p_z$ -orbitals and is occupied by the odd electron to afford a formal Ga–Ga bond order of 1.5. The EPR spectrum<sup>103,105</sup> displayed hyperfine coupling to two different galliums, which resulted in a 64-line spectrum. The hyperfine coupling constants  $a_1(^{69}Ga/^{71}Ga) = 50/64$  G and  $a_2(^{69}Ga/^{71}Ga) = 32/41$  G were in the range observed for the gallium monoanions above. The larger coupling is probably due to Ga(1), although this is not known with certainty.

Solutions of  $R_2^*AlAIR_2^*$  ( $R = -SiBu'_3$ ) in alkanes displayed a simple room-temperature EPR spectrum due to the radical  $R^*AlAIR_2^*$ .<sup>104</sup> The radical may be generated in better yield by thermolysis at 50°C. The coupling to the two  $^{27}Al$  nuclei led to groups of peaks that had from one to six EPR lines with anisotropic broadening of the outer members. Analysis of the splitting yielded the coupling constants  $a_1(^{27}Al) = 21.8$  G and  $a_2(^{27}Al) = 18.9$  G. Although the detailed structure of this radical has not been experimentally determined, DFT calculations afforded an Al–Al bond length of 2.537 Å. It has also been shown that  $R^*MMR_2^*$  ( $M = Al$  or  $Ga$ ) radicals can be reduced to the anions  $[R^*MMR_2^*]^-$ , which contain formal MM double bonds.<sup>104</sup>

By thermolyzing  $R_2^*AlAIR_2^*$  to 100 °C, the trimetallic radical  $\cdot Al_3R_4^*$  was obtained and crystallized.<sup>104</sup> An X-ray crystal structure analysis showed that the aluminums are located at the corners of a triangle

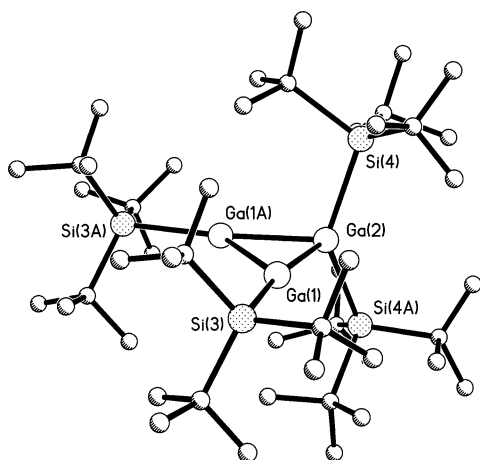


**Figure 8.** Schematic drawing of the structure of the  $\cdot\text{Ga}_3\text{R}_4^*$  radical.<sup>105</sup>

in which one aluminum binds two  $\text{R}^*$  groups and is thus four coordinate. The remaining aluminums bind one  $\text{R}^*$  each, and one has approximately planar and the other pyramidal coordination. The Al–Al distances are in the range 2.703(3)–2.776(2) Å. The resolution of the EPR spectrum is lower than that of  $\text{R}^*\text{AlAIR}_2^*$ , which led to difficulties with analysis. However, it appears that the coupling constant for one of the aluminums is ca. 3 G, and couplings to the remaining aluminums are different but are near 13 G. These values imply that the unpaired electron is predominantly a  $\pi$ -radical. Conventional electron counting suggests that there are five electrons available for the metal–metal bonding in the  $\text{Al}_3$  cluster, implying relatively weak Al–Al bonding with a formal bond order  $< 1$ . The long Al–Al bonds and the nonequivalence of each of the three-coordinated aluminums are also consistent with the existence of a cyclo  $\rightleftharpoons$  catena equilibrium in which one of the Al–Al bonds is broken.

It has also been shown that the corresponding  $\cdot\text{Ga}_3\text{R}_4^*$  species can be synthesized by oxidation of  $[\text{R}_2^*\text{Ga}–\text{GaR}^*–\text{GaR}^*]^-$  or by the reaction of  $\text{R}^*\text{GaGaR}_2^*$  with  $\text{R}^*\text{Br}$ .<sup>105</sup> Unlike the aluminum compound, the  $\cdot\text{Ga}_3\text{R}_4^*$  radical (Figure 8) possesses a quasi-catena structure in the solid state. The Ga–Ga distance between the galliums that carry one  $\text{R}^*$  substituent is ca. 0.37 Å longer than the other two [2.879(1) vs 2.513 Å]. This shows that the two  $\text{GaR}^*$  pairs are more weakly bound to each other than to the  $\text{GaR}_2^*$  moiety, which is not the case with the  $\text{Al}_3\text{R}_4^*$  species. It was concluded that cyclization of the  $\cdot\text{Al}_3\text{R}_4^*$  species is stopped at the halfway stage. As with the  $\text{R}^*\text{MMR}_2^*$  radicals, it is also possible to reduce  $\cdot\text{M}_3\text{R}_4^*$  ( $\text{M} = \text{Al}, \text{Ga}$ ) to the anions  $[\text{M}_3\text{R}_4^*]^-$ , and the structure of the gallium anion has been determined.<sup>105</sup>

### III. Group 14 Element Radicals

A variety of heavier group 14 element-centered radicals have been studied for many years. Among these are the neutral species  $\cdot\text{MR}_3$  and  $\cdot\text{MR}_5$ , the radical cations  $\text{MR}_4^+$  and  $\text{R}_3\text{MMR}_3^+$ , and the radical anions  $\text{MR}_4^-$  and  $\text{R}_3\text{MMR}_3^-$ .<sup>22</sup> Of the heavier group 14 element radicals listed above, only the  $\cdot\text{MR}_3$  species are currently represented by persistent or

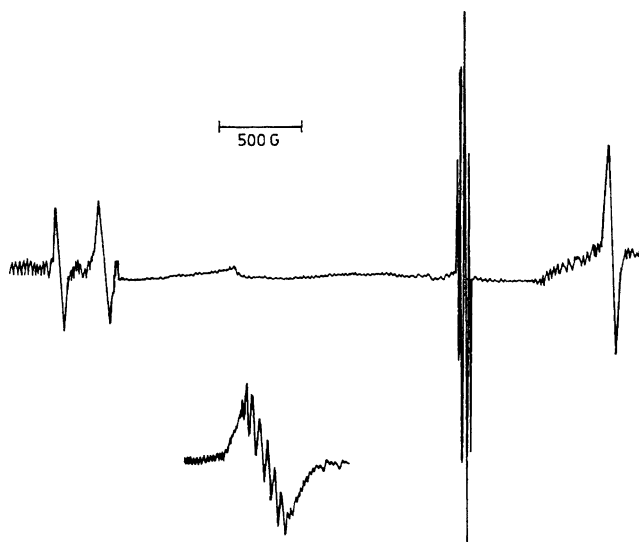
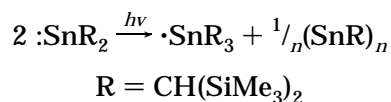


**Figure 9.** Illustration of the EPR spectrum of  $\cdot\text{Sn}\{\text{CH}(\text{SiMe}_3)_2\}_3$ .<sup>108</sup>

stable examples.<sup>24,26,106,107</sup> In these, longevity was induced principally by steric effects, although there can be some delocalization in aryl- or silyl-substituted species. More recent results have featured different types of radicals, both ionic and neutral, in which there is delocalization over two or more group 14 elements. These compounds have enabled the first X-ray crystal structures of heavier group 14 radicals to be determined.

### A. $\cdot\text{MR}_3$ Radicals and Related Species

The first persistent heavier main-group 14 element radicals were discovered during attempts to establish whether the interesting carbene analogue  $:\text{Sn}\{\text{CH}(\text{SiMe}_3)_2\}_2$  existed as a singlet or triplet in the ground state.<sup>24,106,108</sup> It was found that the EPR spectrum (Figure 9) of a solution of  $:\text{Sn}\{\text{CH}(\text{SiMe}_3)_2\}_2$  displayed a weak signal centered near  $g = 2$ . It had a quartet 1:3:3:1 hyperfine structure [ $a(^1\text{H}) = 2.1$  G] that suggested the presence of the  $\cdot\text{Sn}\{\text{CH}(\text{SiMe}_3)_2\}_3$  radical, in which the three equivalent  $\alpha$ -hydrogens were coupled to the unpaired electron. Irradiation of the solution with UV or visible light resulted in a large increase in signal strength, which was not accompanied by the deposition of a tin mirror. The increased signal intensity also allowed the observation of the satellite peaks due to coupling to the  $^{117}\text{Sn}$  ( $I = 1/2$ , 7.68%) and  $^{119}\text{Sn}$  ( $I = 1/2$ , 8.58%) nuclei. Large  $a(^{117}\text{Sn})$  and  $a(^{119}\text{Sn})$  coupling constants of 1697.8 and 1776 G, respectively, were observed, which showed that the unpaired electron was located in an orbital with significant s-character, consistent with pyramidal tin coordination. On the basis of EPR signal intensities, the  $t_{1/2}$  of the  $\cdot\text{Sn}\{\text{CH}(\text{SiMe}_3)_2\}_3$  radical was estimated to be ca. 1 year. It is tempting to view the generation of this radical as a disproportionation reaction as described by



in which the coproduct is the Sn(I) cluster  $(\text{SnR})_n$ .



However, neither the Sn(III) radical nor the  $(\text{SnR})_n$  cluster has been isolated. In addition, experiments on the generation of the corresponding  $\cdot\text{SiR}_3$  and  $\cdot\text{GeR}_3$  radicals do not support the widespread applicability of this route for the heavier group 14 elements.<sup>108</sup> Attempts to generate the lead radical  $\cdot\text{PbR}_3$  resulted in a complex EPR spectrum due to  $\cdot\text{CH}(\text{SiMe}_3)_2$  as well as deposition of a lead mirror.<sup>108</sup>

The radicals  $\cdot\text{SiR}_3$  and  $\cdot\text{GeR}_3$  [ $\text{R} = \text{CH}(\text{SiMe}_3)_2$ ] were detected in solutions formed by treatment of  $\text{Si}_2\text{Cl}_6$  or  $\text{GeCl}_2$ ·dioxane with  $\text{LiR}$ .<sup>108</sup> Their EPR spectra also displayed couplings to the  $\alpha$ -hydrogens  $a(^1\text{H}) = 4.8$  ( $\cdot\text{SiR}_3$ ) and 3.8 G ( $\cdot\text{GeR}_3$ ), as well as  $a(^{29}\text{Si}, I = 1/2, 4.67\%) = 193$  G and  $a(^{73}\text{Ge}, I = 9/2, 7.8\%) = 92$  G. The silicon radical possessed a  $t_{1/2} = \text{ca. } 10$  min at 30 °C, whereas the EPR signals for  $\cdot\text{GeR}_3$  displayed no change in intensity after 4 months. In addition to the alkyl-substituted radicals, the isoelectronic amido species  $\cdot\text{Ge}\{\text{N}(\text{SiMe}_3)_2\}_3$  and  $\cdot\text{Sn}\{\text{N}(\text{SiMe}_3)_2\}_3$  could be generated by similar methods.<sup>107</sup> These displayed couplings to the nitrogen substituents as well as to germanium and tin, and their  $t_{1/2}$  values were >5 months and ca. 3 months, respectively. It is noteworthy that the  $a(^{73}\text{Ge})$  and  $a(^{117/119}\text{Sn})$  of 171 and 3176/3426 G, respectively, are almost double those of the alkyl species, indicating increased s-character for the unpaired electron and a more pyramidal geometry at germanium and tin. This may be a result of the greater electronegativity of the substituents, which tends to increase the p-character of the orbitals employed by the central element for ligand bonding. This increases the s-character of the unpaired electron orbital and, in consequence, the coupling to the  $^{117/119}\text{Sn}$  nuclei.

In the wake of these results, several other persistent germanium- or tin-centered radicals with half-lives that vary from minutes to years were generated. Radicals with a variety of bulky substituents, such as  $-\text{CH}_2\text{CMe}_2\text{Ph}$ ,<sup>109</sup>  $-\text{CH}_2\text{CMe}_3$ ,<sup>110</sup>  $\text{CH}_2\text{SiMe}_3$ ,<sup>110</sup>  $-\text{C}_6\text{H}_2-2,4,6-\text{Me}_3$ ,<sup>111-115</sup>  $-\text{C}_6\text{H}_3-2,6-\text{Me}_2$ ,<sup>121</sup>  $-\text{C}_6\text{H}_2-2,4,6-\text{Et}_3$ ,<sup>114</sup>  $-\text{C}_6\text{H}_2-2,4,6-\text{Pr}^i_3$ ,<sup>114-119</sup> 1-adamantyl,<sup>115</sup>  $-\text{N}(\text{GeMe}_3)_2$ ,<sup>119</sup> and  $-\text{N}(\text{GeEt}_3)_2$ , were obtained.<sup>119</sup> Recent work has shown that highly persistent silyl radicals<sup>120</sup> of the type  $\cdot\text{Si}(\text{SiMe}_3-n\text{Et})_3$  ( $n = 1, 2, \text{ or } 3$ ),<sup>121</sup>  $\cdot\text{Si}(\text{SiPr}^i_3)_3$ ,<sup>122</sup>  $\cdot\text{Si}(\text{SiMe}_2\text{Bu})_3$ ,<sup>123</sup> and  $\text{Si}(\text{SiMe}_2\text{SiMe}_3)_3$ <sup>124</sup> could be synthesized by hydrogen abstraction from the silane, or by oxidation or reduction of the sodium or halide derivatives in solution. Other persistent silyl radicals have been generated by UV irradiation of polydialkylsilanes,  $(\text{R}_2\text{Si})_n$ , in solution.<sup>125</sup> These radicals were stable in the absence of air for several days. The radicals produced were of two types, which involved silicon centers connected either to two neighboring silyl groups of the polymer chain and an alkyl carbon or to three silyls. A mechanism for their formation was also proposed. Very recently, the first structures of stable silyl radicals were reported. The cyclotetrasilanyl species

$[(\text{Bu}^t_2\text{MeSi})\text{SiSi}(\text{SiMeBu}^t_2)\text{Si}(\text{SiMeBu}^t_2)\text{SiBu}^t_2]$  was synthesized by the reduction of the corresponding cyclotetrasilanylium ion with  $\text{NaSiBu}^t_3$  or  $\text{KC}_8$ .<sup>126</sup> It had an almost planar array of four silicons, three of which are trigonally coordinated with essentially planar geometry and involve short Si–Si bonds [2.246(1) and

2.263(1) Å]. The EPR signal ( $g = 2.0058$ ) displayed hyperfine coupling in the form of five doublet satellites. Three doublets have relatively large couplings of 40.7, 37.4, and 15.5 G, consistent with delocalization over the planar  $\text{Si}_3$  allyl-like fragment. This structure was followed by those of  $\cdot\text{Si}(\text{SiMeBu}^t_2)_3$  and its germanium analogue,  $\cdot\text{Ge}(\text{SiMeBu}^t_2)_3$ . These radicals have planar geometries at silicon and germanium, and their EPR data were consistent with the location of the unpaired electron in a p-orbital.<sup>127</sup>

Some EPR data for the currently known persistent or stable heavier group 14 element radicals are presented in Table 2. The half-lives of some of the radicals were not specifically cited in the literature, although in most cases the spectral data were recorded at room temperature. An example of the high stability of some heavier  $\text{MR}_3$  radicals is given by  $\cdot\text{Sn}(\text{C}_6\text{H}_2-2,4,6-\text{Pr}^i_3)_3$  (i.e.,  $\cdot\text{SnTrip}_3$ ), which exists in equilibrium with the Sn–Sn bonded dimer in hydrocarbon solution at room temperature. In effect, its dissociation behavior resembles that of the Gomberg radical  $\cdot\text{CPh}_3$ , and thermal dissociation studies on this molecule and its less crowded congeners involving the  $-\text{C}_6\text{H}_2-2,4,6-\text{Me}_3$  (Mes) and  $-\text{C}_6\text{H}_2-2,4,6-\text{Et}_3$  substituents underline the dramatic effects that the steric crowding has on the Sn–Sn bond strength.<sup>116</sup> For the methyl-substituted (i.e., Mes) species, a  $\Delta H_{\text{diss}}$  of 49(2) kcal mol<sup>-1</sup> was estimated for the Sn–Sn bond, whereas the values for the Et and Pr<sup>i</sup> aryl derivatives were 26.6(2.0) and 8.5(1) kcal mol<sup>-1</sup>. In addition, variable-temperature data for the  $\cdot\text{SnTrip}_3$  radical showed that the hyperfine coupling to  $^{119}\text{Sn}$  decreases markedly with increasing temperature, indicating that the radical has pyramidal geometry.<sup>117</sup> If the geometry were planar, the hyperfine splitting constant would be expected to increase with increasing temperature, since increasing the amplitude of the out-of-plane vibration increases the s-character of the singly occupied orbital, which, in turn, is proportional to the isotropic interaction. A frozen (–140 °C) toluene solution EPR spectrum allowed the  $a_{\parallel}$ ,  $a_{\perp}$ ,  $g_{\parallel}$ , and  $g_{\perp}$  components of the axially symmetric A and g tensors to be determined. These data yielded an out-of-plane angle ( $\theta$ ) of 12.7°, which implied greater planarity than in  $\cdot\text{SnPh}_3$  ( $\theta = 13.6^\circ$ ) due to the size of the Trip groups.

Other studies have dealt with conformational aspects of the radicals.<sup>113</sup> For example, EPR spectra of  $\cdot\text{Ge}(\text{Me})(\text{CH}_2\text{CMe}_3)_2$  and  $\cdot\text{Ge}(\text{Me})(\text{CH}_2\text{SiMe}_3)_2$  showed that two kinds of  $\text{CH}_2$  hydrogens were present due to restricted rotation, whereas fast rotational interconversion among the three preferred conformations of  $\cdot\text{Ge}(\text{CH}_2\text{CMe}_3)_3$  and  $\cdot\text{Ge}(\text{CH}_2\text{SiMe}_3)_3$  effected the equivalence of the six  $\text{CH}_2$  protons.<sup>113</sup> Similarly, variable-temperature EPR studies of  $\cdot\text{M}\{\text{CH}_2\text{CMe}_2\text{Ph}\}_3$  ( $\text{M} = \text{Ge or Sn}$ ) showed that the methylene protons were inequivalent owing to hindered rotation around the Me–C bonds.<sup>111,118</sup> EPR studies of the aryl-substituted germanium radicals such as  $\cdot\text{GeMes}_3$  showed that there is spin delocalization through conjugation of the germanium p-orbital with the p-orbitals of the aryl substituents.<sup>111-114</sup> Although all of the Ge and Sn radicals are pyramidal, the recently characterized  $\cdot\text{Si}(\text{SiR}_3)_3$

Table 2. Some EPR and Stability Data for  $\cdot\text{MR}_3$  Radicals (M = Si, Ge, or Sn)

radical	g	$a(^{29}\text{Si})^a$	a(X)	$t_{1/2}^b$	refs	g	$a(^{73}\text{Ge})$	a(X)	$t_{1/2}$	refs	g	$a(^{117/119}\text{Sn})$	a(X)	$t_{1/2}$	refs
$\cdot\text{M}\{\text{CH}(\text{SiMe}_3)_2\}_3$	2.0027	193	4.8 (3H)	10 min	108	2.0078	92	3.8 (3H)		108	2.0094	1698, 1776	2.1 (3H)	ca. 1 y	108
$\cdot\text{M}\{\text{N}(\text{SiMe}_3)_2\}_3$						1.9991	171	10.6 (3N)	> 5 mo	108	1.9912	3176, 3426	10.9 (3N)	ca. 3 mo.	108
$\cdot\text{M}\{\text{N}(\text{Bu})^t(\text{SiMe}_3)\}_3$						1.9998	173	12.9 (3N)	ca. 5 min	108	1.9928		12.7 (3N)	ca. 5 min	108
$\cdot\text{M}\{\text{N}(\text{GeMe}_3)_2\}_3$						1.9994	14.5	11.0 (3N)	ca. 22 h	119	1.9924		10.7 (3N)	ca. 10 h	119
$\cdot\text{M}\{\text{N}(\text{GeEt}_3)_2\}_3$											1.9939			ca. 10 h	119
$\cdot\text{M}\{\text{C}_6\text{H}_2-2,4,6-\text{Me}_3\}_3$	2.0027	135	0.7	20 s	111, 115	2.0084	68.4	6.9 (3N)	> 24 h	111, 112	2.0086				115, 116
$\cdot\text{M}\{\text{C}_6\text{H}_2-2,4,6-\text{Et}_3\}_3$											2.0076				115, 116
$\cdot\text{M}\{\text{C}_6\text{H}_2-2,4,6-\text{Pr}^i\}_3$											2.0078	1602, 1678			115-117
$\cdot\text{M}(\text{CH}_2\text{CMe}_2\text{Ph})_3$						2.0096		5.1 (6H)		115	2.0150	1325, 138	3.1		110
$\cdot\text{M}(\text{CH}_2\text{CMe}_2)_3$						2.0107		5.14 (6H)		115	2.0145	0			
$\cdot\text{M}(\text{SiMe}_3)_3$	2.0053	63.8	7.1	1 s ( $-20^\circ\text{C}$ )	120						2.0170		3.4 (6H)		110, 118
$\cdot\text{M}(\text{SiEtMe}_2)_3$	2.0060	62.8	7.1	3 h	121										
$\cdot\text{M}(\text{SiEt}_2\text{Me})_3$	2.0060	60.3	7.1	1 d	122										
$\cdot\text{M}(\text{SiEt}_3)_3$	2.0063	57.2	7.1	1.5 mo	122										
$\cdot\text{M}(\text{SiPr}^i)_3$	2.0061	55.6	8.1	indefinitely stable	122										
$\cdot\text{M}(\text{SiMe}_2\text{Bu}^t)_3$	2.060	56.9	9.0	indefinitely stable	123										
$\cdot\text{M}(\text{SiMe}_2\text{SiMe}_3)_3$	2.0065	59.9	8.1	6 min	124										
$\cdot\text{M}(\text{SiMeBu}^t)_3$	2.0056	58.0	7.9	stable as crystals	127	2.0229	20.0	7.3 (3Si)		127					

<sup>a</sup> Hyperfine coupling constants are given in gauss. <sup>b</sup> s, seconds; min, minutes; h, hours; d, days; mo, months; y, year.

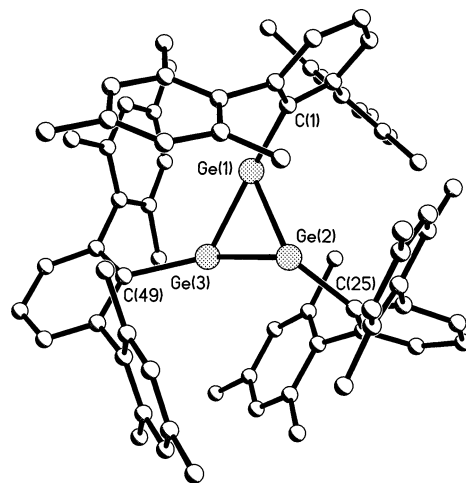
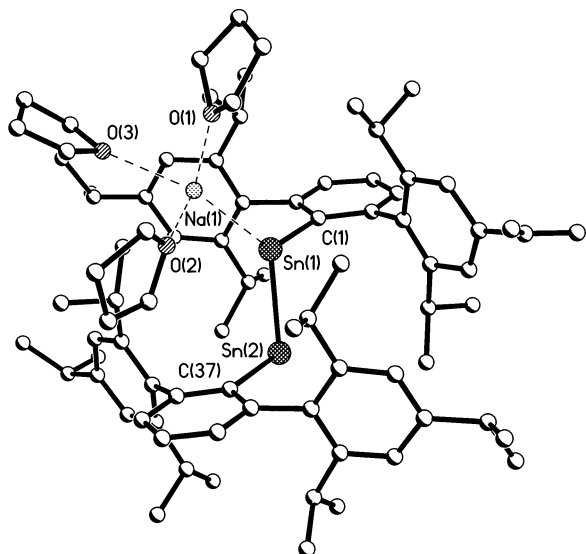


Figure 10. Schematic drawing of the structure of  $\cdot(\text{GeC}_6\text{H}_3-2,6-\text{Mes}_2)_3$ .<sup>126</sup>

radicals<sup>121–123</sup> show that they have planar geometries, with  $a(^{29}\text{Si})$  hyperfine couplings of ca. 60 G. These values are ca. one-third of that observed for  $\cdot\text{Si}(\text{CH}(\text{SiMe}_3)_2)_3$ ,<sup>108</sup> which was presumed to have pyramidal coordination with s-character in the unpaired electron orbital. These radicals are highly persistent, and it seems likely that they can be isolated and crystallized as stable species.

## B. Multinuclear Radicals and Radical Anions

Reduction of the divalent Ge(II) species  $\text{Ge}(\text{Cl})(\text{C}_6\text{H}_3-2,6-\text{Mes}_2)$  with  $\text{KC}_8$  afforded the trimer  $\cdot(\text{GeC}_6\text{H}_3-2,6-\text{Mes}_2)_3$  as blue crystals.<sup>128</sup> It represented the first structure of a neutral heavier group 14 element-centered radical, and the X-ray data showed that it crystallized as well-separated molecules that had a cyclic triangular arrangement of three germaniums (Figure 10). The average Ge–Ge distance is 2.35(7) Å, consistent with some multiple Ge–Ge bonding (cf. 2.44 Å for a Ge–Ge single bond). Although the structure had disorder, it could be refined to an overall residual ( $R_1$ ) value of 0.064. The presence of a disordered core unit is consistent with its formulation as a cyclogermanenyl radical in which the unpaired electron could be located on each germanium with equal probability. Since the substituent at each germanium is the same, the molecule may adopt three orientations with very little difference in appearance at its periphery. In the crystal, the germanium bearing the unpaired electron may be randomly distributed over three positions in the ring. Furthermore, since a pyramidal coordination geometry is expected for the germanium carrying the unpaired electron and the doubly bonded germaniums should have planar coordination, the disorder could be expected to produce slightly different germanium positions in each case. The EPR spectrum in hexane solution displayed a signal at  $g = 2.0069$  as well as hyperfine  $a = 16$  G coupling to  $^{73}\text{Ge}$  ( $I = 9/2$ , 7.8%). The intensity of the hyperfine lines in the EPR spectrum was consistent with the location of the unpaired electron at one germanium, although delocalization cannot be ruled out. The coupling constant was consistent with the location of the electron in an orbital with little s-character, i.e., a  $\pi$ -orbital—



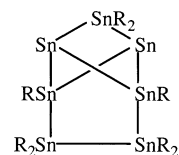
**Figure 11.** Schematic drawing of the X-ray crystal structure of  $(\text{THF})_3\text{NaAr}^*\text{SnSnAr}^*$  ( $\text{Ar}^* = \text{C}_6\text{H}_3\text{-2,6-Trip}_2$ ).<sup>130b</sup>

possibly a doubly degenerate, antibonding  $e$  level. Further reduction of the radical is possible by reaction with another equivalent of  $\text{KC}_8$ . In this case, the  $\text{Ge}_3$  ring is opened to produce the catena structure  $\text{K}(\text{GeC}_6\text{H}_3\text{-2,6-Mes}_2)_3$ , which is electronically analogous to an allyl anion in a  $Z$ -configuration.<sup>128</sup>

Reduction of the corresponding tin halide,  $\text{Sn}(\text{Cl})(\text{C}_6\text{H}_3\text{-2,6-Mes}_2)$ , did not afford an isolable radical but produced a red solution from which the diamagnetic cluster  $\text{Sn}_8(\text{C}_6\text{H}_3\text{-2,6-Mes}_2)_4$  could be isolated.<sup>129</sup> However, reduction of the more sterically crowded halide  $\text{Sn}(\text{Cl})(\text{C}_6\text{H}_3\text{-2,6-Trip}_2)$  [i.e.,  $\text{Sn}(\text{Cl})\text{Ar}^*$ ] with  $\text{KC}_8$  yielded the crystalline, dark red, solvent-separated ion pairs  $[\text{K}(\text{THF})_6][\text{Ar}^*\text{SnSnAr}^*]$  and  $[\text{K}(\text{dibenzo-18-crown-6})(\text{THF})_2][\text{Ar}^*\text{SnSnAr}^*] \cdot 2\text{THF}$  ( $\text{Ar}^* = \text{C}_6\text{H}_3\text{-2,6-Trip}_2$ ).<sup>130a</sup> In THF at room temperature, the EPR spectra of the two compounds were essentially identical, with signals at  $g = 2.0069$  and hyperfine couplings to  $^{117}\text{Sn}$  and  $^{119}\text{Sn}$  of  $a(^{117/119}\text{Sn}) = 8.3/8.5$  G, consistent with the location of the unpaired electron in a  $p$ - or  $\pi$ -orbital. X-ray crystallography showed that the  $[\text{Ar}^*\text{SnSnAr}^*]^-$  radical anion is trans-bent, with  $\text{Sn-Sn}$  distances of 2.8123(9) and 2.7821(14) Å and  $\text{Sn-Sn-C}$  angles of 95.2(1) and 97.3(2)°. These structural parameters are consistent with a lone pair at each tin and the metals  $\sigma$ -bonded as a result of overlap of tin 5 $p$ -orbitals. The unpaired electron occupies a  $\pi$ -orbital formed by side-on overlap of two tin 5 $p$ -orbitals to give a formal  $\text{Sn-Sn}$  bond order of 1.5. Yet, the average  $\text{Sn-Sn}$  bond length of 2.806(16) Å is close to the  $\text{Sn-Sn}$  single bond distance in gray tin (2.80 Å). The observed  $\text{Sn-Sn}$  bond length suggests that the  $\pi$ -bond is weak. However, it is probable that a single  $\text{Sn-Sn}$  bond, formed by end-on overlap of tin 5 $p$ -orbitals, would be significantly longer than the 2.80 Å seen for tetrahedrally coordinated tins in elemental tin. In this way, the measured  $\text{Sn-Sn}$  bond length may actually represent a significant shortening. A later structural determination of the contact ion pair  $(\text{THF})_3\text{NaAr}^*\text{SnSnAr}^*$  (Figure 11) displayed a  $\text{Sn-Sn}$  bond length of 2.817(13) Å, which is essentially identical to those

cited above.<sup>130b</sup> The  $\text{Na}^+$  ion, which is solvated by three THF molecules, interacts with one of the tin atoms in a terminal fashion, with a  $\text{Na-Sn}$  distance of 3.240(7) Å. The (ipso) $\text{C-Sn-Sn-C}$ (ipso) array is planar, and the  $\text{C-Sn-Sn}$  angles are 97.9(3) and 98.0(4)°, slightly wider than the angles in the solvent-separated ion pairs. In general, the observed structure supports the bonding model given above, and the coordination of the  $\text{Na}^+$  ion to one of the tins at the position expected for the lone pair lends credence to the presence of a nonbonding pair of electrons at this site. It is also possible to reduce the tin mono-anion further to give the formally double-bonded species  $\text{K}_2\text{Ar}^*\text{SnSnAr}^*$ ,<sup>131</sup> in which the dianion is isoelectronic to the known neutral species  $\text{Ar}^*\text{-SbSbAr}^*$ .<sup>132</sup> A corresponding germanium species,  $\text{Na}_2\text{-Ar}^*\text{GeGeAr}^*$ ,<sup>131</sup> is also known.

Radical anions of the formula  $[\text{ER}_2]^-$  ( $\text{E} = \text{Ge}$  or  $\text{Sn}$ ) represent another class of potentially stable group 14 element radicals. These species were first detected during the reduction of the cyclotristannane  $c\text{-}\{\text{Sn}(\text{C}_6\text{H}_3\text{-2,6-Et}_2)_2\}_3$  with lithium metal, during which the radical anion  $[\text{Sn}(\text{C}_6\text{H}_3\text{-2,6-Et}_2)_2]^-$  was observed as an intermediate at room temperature by EPR spectroscopy.<sup>133</sup> The anions  $[\text{E}\{\text{CH}(\text{SiMe}_3)_2\}_2]^-$  were synthesized by reduction of the dialkyls with sodium in THF.<sup>134</sup> The  $[\text{Ge}\{\text{CH}(\text{SiMe}_3)_2\}_2]^-$  species is persistent at room temperature. The EPR spectrum has a signal ( $g = 2.0125$ ) with a 1:2:1 triplet pattern due to coupling to two  $\alpha$ -hydrogens [ $a(^1\text{H}) = 2.6$  G]. At higher gain, four weak satellite lines were observed at both sides of the central peak, due to coupling ( $a = 12.5$  G) to  $^{73}\text{Ge}$  ( $I = 9/2$ , 7.8%). For the tin radical in THF at  $-80^\circ\text{C}$ , the EPR parameters are  $g = 2.0094$  and  $a(^{119,121}\text{Sn}) = 116$  G. The small values of the couplings to the central elements in both spectra are consistent with the location of the unpaired electron in a  $p$ -orbital. Thermal decomposition of  $c\text{-}\{\text{Sn}(\text{C}_6\text{H}_3\text{-2,6-Et}_2)_2\}_3$  also produced the cluster species **IX** in low yield, which could be singly reduced



**IX**

to give the corresponding radical anion, which displayed a single resonance at  $g = 1.95$ . This could be satisfactorily simulated by assuming hyperfine interaction with three sets of equivalent tin atoms with the following parameters:  $a(^{119/117}\text{Sn}) = 22$  G (two Sn atoms),  $a(^{119/117}\text{Sn}) = 50$  G (two Sn atoms),  $a(^{119/117}\text{Sn}) = 65$  G (three Sn atoms), line width = 6.5 G. This simulation showed that the framework retains its integrity upon reduction.<sup>133</sup>

Another class of anionic radicals arises from the reduction of  $\text{R}_2(\text{X})\text{SiSi}(\text{X})\text{R}_2$  ( $\text{X} = \text{Cl}, \text{Br}, \text{or I}$ ;  $\text{R} = \text{Pr}^i$  or  $\text{Bu}^i$ ) with  $\text{Na/K}$  to afford the disilylenyl anions  $[\text{R}_2\text{SiSiR}_2]^-$ .<sup>135</sup> They are stable for several minutes at room temperature where  $\text{R} = \text{Bu}^i$  and display an  $a(^{29}\text{Si})$  hyperfine coupling of 33.6 G. On the other hand, reduction of  $\text{Mes}_2(\text{Cl})\text{SiSi}(\text{Cl})\text{Mes}_2$  with an

**Table 3. EPR Parameters and Half-Lives for Long-Lived Phosphinyl and Arsinyl Radicals**

radical	$a(\text{E})^a$	$a(\text{H})$	$a(^{14}\text{N})$	$g_{\text{av}}$	$t_{1/2}$	refs
$:\dot{\text{P}}\{\text{CH}(\text{SiMe}_3)_2\}_2$	96.3	6.4		2.009	> 1 y	25, 151
$:\dot{\text{P}}\{\text{N}(\text{SiMe}_3)_2\}_2$	91.8			2.008	ca. 5 d	25, 151
$:\dot{\text{P}}\{\text{CH}(\text{SiMe}_3)_2\}\{\text{N}(\text{SiMe}_3)_2\}$	93.0	8.1		2.008	ca. 10 d	151
$:\dot{\text{P}}\{\text{CH}(\text{SiMe}_3)_2\}\{\text{NPr}^t\}_2$	63.0		3.7	2.005	ca. 1 d	151
$:\dot{\text{P}}\{\text{NPr}^t\}_2\{\text{N}(\text{SiMe}_3)_2\}$	77.2		5.2	2.007	ca. 1 d	151
$:\dot{\text{P}}\{\text{N}(\text{Bu}^t)(\text{SiMe}_3)_2\}_2$	101.5			2.007	ca. 5 d	151
$:\dot{\text{P}}\{\text{NPr}^t\}_2\{\text{N}(\text{Bu}^t)(\text{SiMe}_3)\}$	74.0		5.1	2.007	ca. 3 d	151
$:\dot{\text{P}}\{\text{CH}(\text{SiMe}_3)_2\}(\text{NMe}_2)$	65.0			2.008		151
$:\dot{\text{P}}(\text{Mes})\{\text{N}(\text{SiMe}_3)_2\}$	96.7			2.008		151
$:\dot{\text{P}}(\text{Mes}^*)\{\text{CH}(\text{SiMe}_3)_2\}$	104	13.5		2.008		152
$:\dot{\text{P}}(\text{Mes}^*)\text{Ph}$	105			2.007		152
$:\dot{\text{P}}(\text{Mes}^*)\{\text{N}(\text{SiMe}_3)_2\}$	108			2.006		152
$:\dot{\text{P}}(\text{Mes}^*)(\text{OBu}^t)_3$	100			2.005		152
$:\dot{\text{P}}(\text{Mes}^*)(\text{SPr}^t)$	98			2.011		152
$:\dot{\text{P}}(\text{Mes}^*)(\text{OBu}^t)$	99			2.012		152
$:\dot{\text{P}}(\text{Mes}^*)(\text{OMes}^*)$	94			2.066		152
$:\dot{\text{P}}(\text{Mes}^*)_2$	103			2.007		152
$:\dot{\text{P}}(\text{OMes}^*)_2$	82			1.999		152
$:\dot{\text{As}}\{\text{CH}(\text{SiMe}_3)_2\}_2$	37.2			2.040	ca. 10 d	25, 151
$:\dot{\text{As}}\{\text{N}(\text{SiMe}_3)_2\}_2$	31.8			2.038	ca. 15 d	25, 151
$:\dot{\text{As}}\text{Mes}^*_2$	50					152

<sup>a</sup> Hyperfine coupling constants are given in gauss.

electron-rich olefin afforded the chloro-bridged radical,



which displayed  $a(^{29}\text{Si}) = 120$  G and a quartet pattern  $a(\text{Cl}) = 7.4$  G. Unfortunately, no other multiply bonded, heavier group 14 element radicals similar to these have been reported.

The nine-atom polyhedra  $\text{M}_9^{3-}$  ( $\text{M} = \text{Ge}, \text{Sn}, \text{or Pb}$ ) were the first stable group 14 element molecular ion radicals to be isolated.<sup>136,137</sup> They have been characterized by X-ray crystallography, magnetic studies, and EPR spectroscopy.<sup>136–142</sup> EPR measurements on crystals of  $[\text{K}(\text{2.2.2})]_6^+[\text{Ge}_9\text{Ge}_9]^{6-}(\text{en})_{0.5}$  ( $\text{en} = 1,2$ -ethylenediamine) and  $[\text{K}(\text{2.2.2})]_6^+[\text{Sn}_9\text{Sn}_9]^{6-}(\text{en})_{1.5}(\text{PhMe})_{0.5}$  show that they contain paramagnetic  $[\text{M}_9]^{3-}$  clusters with one unpaired electron.<sup>141,142</sup> However, the  $\text{Ge}_9^{3-}$  clusters in  $[\text{K}(\text{2.2.2})]_6^+[\text{Ge}_9\text{Ge}_9]^{6-}(\text{en})_{2.5}$  have different shapes, which led to the assumption that  $[\text{Ge}_9]^{4-}$  and  $[\text{Ge}_9]^{2-}$  were present. Magnetic studies on the species  $[\text{K}(\text{2.2.2})]_6^+[\text{M}_9\text{M}_9]^{6-}(\text{en})_{1.5}(\text{PhMe})_{0.5}$  ( $\text{M} = \text{Sn}$  or  $\text{Pb}$ ) displayed magnetic moments of  $\mu = 1.25$  and  $1.07 \mu_{\text{B}}$  for tin and lead, which are below the values expected for one unpaired electron.<sup>142</sup> This suggested that about 50% paramagnetic  $[\text{M}_9]^{3-}$  is present as well as the mixed-valence species  $[\text{M}_9]^{2-/4-}$ . The existence of mixed-valent species and the fact that electron transfer can occur between them suggest that they are candidates for use as building blocks in materials.<sup>136</sup>

#### IV. Group 15 Element Radicals

The involvement of phosphorus-centered radicals in many reactions has been recognized for many decades.<sup>22,143</sup> The evidence was based primarily on kinetic and product studies as well as observations which allowed the deduction of plausible reaction schemes that implied the participation of radicals.<sup>143,144</sup> The phosphinyl radical  $:\dot{\text{P}}\text{Ph}_2$  and its

arsenic analogue were detected at low temperatures in 1966.<sup>145</sup> Direct spectroscopic observation of the participation of a phosphorus radical in reactions was reported in 1969, when the EPR spectrum of  $\text{Me}_3\dot{\text{P}}\text{O}(\text{Bu}^t)$  was observed during the displacement of alkyl groups from phosphorus by  $\text{OBu}^t$  radicals.<sup>146</sup> The hyperfine structure showed that one of the methyl groups was distinct from the other two, consistent with a quasi-trigonal bipyramidal geometry. The  $a(^{31}\text{P}, I = 1/2, 100\%)$  value was found to be 618 G, so the location of the unpaired electron at an equatorial site involving considerable s-character in the phosphorus valence orbital was indicated. However, tetravalent phosphoranyl radicals<sup>147</sup> represent just one of several classes of phosphorus radicals<sup>22</sup> that include phosphinyl ( $\dot{\text{P}}\text{R}_2$ ),<sup>148</sup> phosphonyl ( $:\text{O}\dot{\text{P}}\text{R}_2$ ), and phosphoniumyl (or phosphenium) radical cations  $[\cdot\text{PR}_3]^+$ ,<sup>147</sup> radical anions  $[\dot{\text{P}}\text{R}_3]^-$ ,<sup>147</sup> and radicals with more than one phosphorus center.<sup>149</sup> The latter have been reviewed recently,<sup>149</sup> as have the less extensively studied radicals of arsenic, antimony, and bismuth.<sup>150</sup>

The first persistent phosphorus radicals were the isoelectronic phosphinyl species  $:\dot{\text{P}}\{\text{CH}(\text{SiMe}_3)_2\}_2$  and  $:\dot{\text{P}}\{\text{N}(\text{SiMe}_3)_2\}_2$ . They were generated under photolysis in solution by reaction of the dialkyl or diamido halides with an electron-rich olefin.<sup>25</sup> The arsenic species could be generated under similar conditions.<sup>25</sup> The radical  $:\dot{\text{P}}\{\text{CH}(\text{SiMe}_3)_2\}_2$  could also be obtained by reduction of the dialkylphosphorus halide with sodium. These radicals showed no decay in EPR signal intensity after 15 days. Several other long-lived phosphinyl radicals with a variety of substituents could be generated in this way.<sup>151,152</sup> The salient EPR parameters for these radicals as well as their half-lives are listed in Table 3. The main feature of solution EPR spectra of all the phosphorus radicals is the hyperfine coupling to the  $^{31}\text{P}$  nucleus, which results in a doublet which may be further split by coupling to  $\alpha$ -hydrogens or substituent nitrogens. They display  $a(^{31}\text{P})$  values in the range 63–108 G,

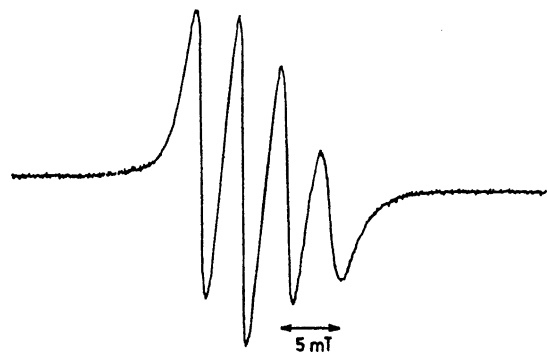


**Figure 12.** EPR spectrum of the radical  $:\text{As}\{\text{CH}(\text{SiMe}_3)_2\}_2$  in toluene at  $27\text{ }^\circ\text{C}$ .<sup>151</sup>

with slightly lower values usually observed for the nitrogen- or oxygen-substituted compounds.<sup>152</sup> It is notable that nitrogen hyperfine coupling in the amide-substituted radicals was observed only when the nitrogen substituents were alkyl groups.<sup>151</sup> This feature is also accompanied by lower  $^{31}\text{P}$  couplings. These data were interpreted in terms of increased P–N  $\pi$ -interactions for the dialkyl amido-substituted compounds. This is due to the smaller size of the alkyl groups vis-à-vis the silyl substituents, which permits the coplanar orientation of phosphorus and nitrogen coordination planes. The arsinyl radicals display a quartet hyperfine coupling pattern with broad lines in the intensity ratio 1:1:1:1 (Figure 12).<sup>25,151</sup> This is consistent with coupling of the unpaired electron to  $^{75}\text{As}$  ( $I = 3/2$ , 100%). No coupling to the  $\alpha$ -hydrogens could be resolved. The EPR spectra of the  $-\text{CH}(\text{SiMe}_3)_2$ - and  $-\text{N}(\text{SiMe}_3)_2$ -substituted phosphinyl and arsinyl radicals were also recorded in polycrystalline frozen solution matrices at ca.  $-150\text{ }^\circ\text{C}$ , where relatively large parallel and small perpendicular components were apparent.<sup>151</sup> The values obtained were consistent with work on less stable radical species such as  $:\text{P}(\text{NMe}_2)_2$ ,<sup>152</sup>  $:\text{AsPh}_2$ ,<sup>153</sup> etc. The  $:\text{E}\{\text{CH}(\text{SiMe}_3)_2\}_2$  ( $\text{E} = \text{P}, \text{As}$ ) radicals can be prepared in multigram quantities and can be distilled as red vapors, which dimerize on cooling to give salmon-pink crystalline solids.

More recent investigations have afforded the structural details of the  $:\text{E}\{\text{CH}(\text{SiMe}_3)_2\}_2$  ( $\text{E} = \text{P}$  or  $\text{As}$ ) monomers, which represented the first detailed structural characterization of phosphorus- or arsenic-centered radicals.<sup>155,156</sup> Vapor electron diffraction data showed that both radicals adopted a V-shaped geometry (Figure 13), with C–P–C and C–As–C angles of  $104.0(10)$  and  $101.2(10)^\circ$ , similar to those in the corresponding pnictide salts  $[\text{Li}(\mu\text{-E}\{\text{CH}(\text{SiMe}_3)_2\}_2)]_3$ .<sup>157,158</sup> The P–C and As–C bonds were not elongated despite the large size of the alkyl substituent. The radicals possessed a syn,syn configuration in which the methine (i.e.,  $\alpha$ ) hydrogens were oriented toward the middle of the C–E–C skeleton in order to minimize interligand interactions. This resulted in a structure that displayed only minor distortion in the bond angles within each ligand. In the crystalline phase, the radicals were dimerized through P–P or As–As bonding. These bonds [P–P =  $2.3103(7)$  Å, As–As  $2.538(2)$  Å] are about  $0.1$  Å longer than normal. However, the elongation of these bonds is insufficient to account

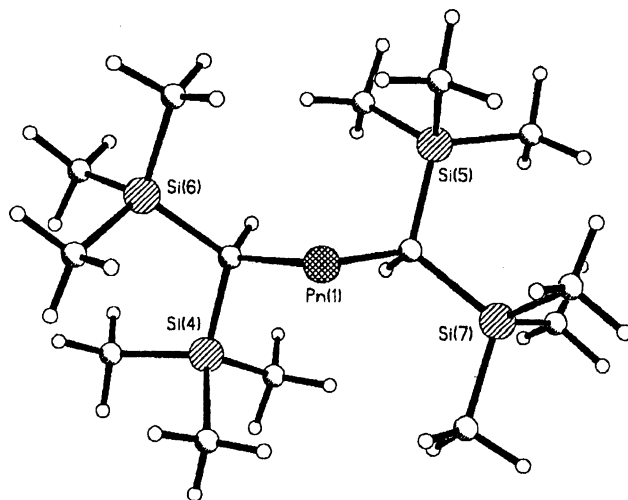


**Figure 13.** Illustration of the vapor-phase structure of the radicals  $:\text{P}\{\text{CH}(\text{SiMe}_3)_2\}_2$  ( $\text{Pn} = \text{P}$  or  $\text{As}$ ).<sup>156</sup>

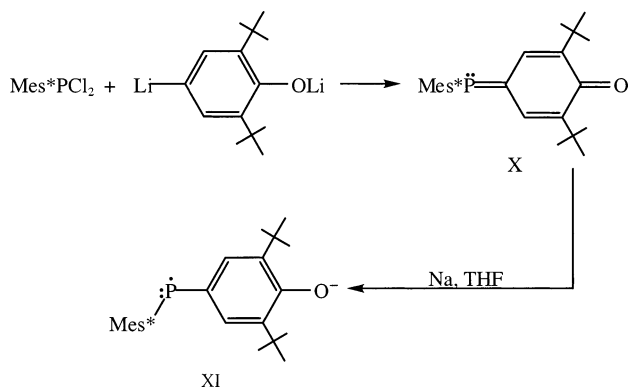
for their ready dissociation in solution or in the vapor phase. Examination of the structural details within the  $-\text{CH}(\text{SiMe}_3)_2$  ligands showed them to have considerable angular distortion. Moreover, the  $-\text{CH}(\text{SiMe}_3)_2$  groups of each  $:\text{ER}_2$  fragment possess a syn,anti orientation which allows more efficient packing in the dimer. This results in more steric strain within each  $-\text{CH}(\text{SiMe}_3)_2$  group and between the  $-\text{CH}(\text{SiMe}_3)_2$  groups attached to each pnictogen as well as between the  $-\text{CH}(\text{SiMe}_3)_2$  groups in each half of the molecule. As a result, the dimerized molecule is analogous to a coiled spring which stores enough energy in the form of strain to cleave a P–P or As–As bond upon dissolution or vaporization. Such conclusions were supported by computations, and the phenomenon was predicted to generally occur in molecules in which the bulky ligands are flexible and capable of undergoing significant conformational change and where there is a bond that has an energy close to the strain energy stored.<sup>156</sup>

Phosphinyl radicals of formula  $:\dot{\text{P}}(\text{Mes}^*)\text{X}$  ( $\text{X} = -\text{OBu}^t, -\text{SPr}^n, -\text{SBu}^t$ ) were produced when the bulky diphosphene  $\text{Mes}^*\text{P}=\text{PMes}^*$  ( $\text{Mes}^* = \text{C}_6\text{H}_3\text{-}2,4,6\text{-Bu}^t$ ) was photolyzed in the presence of  $\text{Bu}^t\text{-OOBu}^t$ ,  $\text{Pr}^n\text{SSPr}^n$ , or  $\text{Bu}^t\text{SSBu}^t$ .<sup>152</sup> Other persistent species of formula  $:\dot{\text{P}}(\text{Mes}^*)\text{X}$  were formed when a toluene solution of  $\text{PMes}^*(\text{X})\text{Cl}$  [ $\text{X} = -\text{Cl}, -\text{Ph}, -\text{Mes}, -\text{OMes}^*, -\text{CH}(\text{SiMe}_3)_2$ ] was photolyzed in the presence of an electron-rich olefin. Similarly, the radical  $:\dot{\text{P}}(\text{OMes}^*)_2$  was obtained from  $:\dot{\text{P}}(\text{OMes}^*)_2\text{Cl}$ . The radical  $:\text{PMes}^*_2$  was prepared by reaction of  $\text{PMes}^*\text{Cl}_2$  with an excess of  $\text{LiMes}^*$ . It is also formed (probably by disproportionation) when a solution of  $:\dot{\text{P}}(\text{Mes}^*)\text{-Cl}$  is stored at room temperature.<sup>152</sup> The arsinyl radical  $:\dot{\text{As}}\text{Mes}^*_2$ , which displayed an EPR signal with a quartet hyperfine structure with  $a(^{75}\text{As}) = 50$  G, could also be obtained. The photolysis of  $\text{Mes}^*\text{-P}=\text{PMes}^*$  in the presence of  $\text{Bu}^t\text{OOBu}^t$  or  $\text{Pr}^n\text{SSPr}^n$  afforded the phosphino phosphinyl radicals  $\text{Mes}^*\text{-}(\text{Bu}^t\text{O})\text{PPMes}^*$  [ $a(^{31}\text{P}/^{31}\text{P}') = 102/44$  G],  $\text{Mes}^*(\text{Pr}^n\text{S})\text{-PPMes}^*$  [ $a(^{31}\text{P}/^{31}\text{P}') = 100/44$  G], or  $:\dot{\text{P}}(\text{Mes}^*)(\text{SPr}^n)$ , in addition to  $:\dot{\text{P}}(\text{Mes}^*)(\text{OBu}^t)$ . A phosphino phosphinyl radical,  $\text{Mes}^*(\text{H})\text{PPMes}^*$ , was also produced by irradiation of single crystals of  $\text{Mes}^*\text{P}=\text{PMes}^*$ , which allowed the various experimental hyperfine tensors

to be compared to those of hypothetical  $\text{H}_2\text{PPH}_2$  and  $\text{Me}(\text{H})\text{PPMe}$ .<sup>159</sup> The calculations showed that the barrier to rotation around the P–P bond in  $\text{H}_2\text{PPH}$  is only 2.8 kcal mol<sup>-1</sup>.

Recent work has shown that a diphosphanil radical can be isolated by reduction of the cation  $[\text{Mes}^*(\text{Me})\text{PPMes}^*]^+$ <sup>160</sup> with the electron-rich olefin  $(\text{Me}_2\text{N})_2\text{-CC}(\text{NMe}_2)_2$ .<sup>161</sup> The EPR spectrum displayed a  $g$  value of 2.006 and coupling to two phosphorus nuclei of 89.3 and 139.3 G. The green-colored radical may be doped into single crystals of the disphosphane  $\text{Mes}^*(\text{Me})\text{-PP}(\text{Me})\text{Mes}^*$ , and the anisotropic <sup>31</sup>P coupling constants could be determined from measurements on these. The doped crystals could be stored at room temperature without decomposition and could even be handled in air. Density functional calculations afforded excellent agreement between calculated and experimental spectroscopic and structural parameters.<sup>160</sup>

The use of the very bulky  $\text{Mes}^*$  substituent has also allowed the preparation of the first stable  $p$ -phosphaquinone<sup>162</sup> via the reduction of the quinoidal species **X**, as shown by



The solution EPR spectrum of **XI** displays a signal at  $g = 2.0069$ , with  $a(^{31}\text{P}) = 93$  G. The EPR spectrum in frozen solution displays large anisotropy of hyperfine coupling, which allowed us to estimate that ca. 64% of the spin density was localized in the phosphorus 3p-orbital, indicating that the canonical form **X** of the radical given above is a major contributor to the overall structure.

Several other classes of phosphorus-centered radicals have been obtained with bulky substituents. Reduction of  $:\dot{\text{P}}(\text{O})(\text{Mes}^*)_2\text{Cl}$  with electron-rich olefin gave the phosphoryl radical  $\text{OP}(\text{Mes}^*)_2$  [ $a(^{31}\text{P}) = 375$  G,  $g = 2.005$ ]. Treatment of  $:\text{PMes}^*\text{Cl}_2$  with  $\text{LiN}(\text{SiMe}_3)_2$  yielded the EPR signal of the phosphorimidoyl radical  $\text{P}\{\text{N}(\text{SiMe}_3)\}\{\text{N}(\text{SiMe}_3)_2\}\text{Mes}^*$  [ $a(^{31}\text{P}) = 336.5$  G,  $a(^{14}\text{N}/^{14}\text{N}') = 5.2/4.0$  G,  $g = 2.0032$ ].<sup>152</sup> Several persistent radicals of this class could be produced by the addition of alkoxy, alkyl, or acyl radicals to the phospho(III)azene  $(\text{Me}_3\text{Si})_2\text{NP}=\text{N}(\text{SiMe}_3)$ .<sup>163</sup> These species were characterized by large  $a(^{31}\text{P})$  values (ca. 250–500 G) and  $a(^{14}\text{N})$  values in the range 4.3–10.6 G. Their lack of reactivity was ascribed to steric shielding by the bulky trimethylsilyl groups.<sup>161</sup>

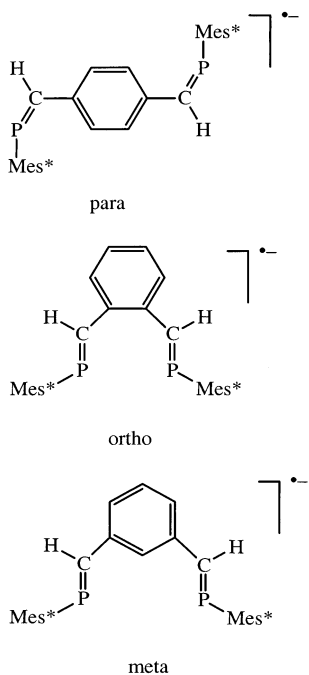
The reaction of  $\text{Mes}^*\text{PPMes}^*$  with sodium naphthalenide affords the radical anion  $[\text{Mes}^*\text{PPMes}^*]^-$ .<sup>152</sup> Electrochemical studies showed that  $\text{Mes}^*\text{PP-}$

$\text{Mes}^*$ ,<sup>164,165</sup> as well as  $(\text{Me}_3\text{Si})_3\text{CEEC}(\text{SiMe}_3)_3$  ( $\text{E} = \text{P}$  or  $\text{As}$ ),<sup>156</sup> underwent quasi-reversible one-electron reductions to generate the corresponding anions in solution. The solution EPR spectra of the diphosphene anions at room temperature display a 1:2:1 triplet hyperfine coupling pattern, indicating equal interactions with two phosphorus nuclei. The  $a(^{31}\text{P}, 2\text{P})$  and  $g$  values were 43 G, 2.018 and 55 G, 2.013, indicating that the unpaired electron was in an orbital of  $\pi$ -symmetry, (i.e., a  $\pi^*$ -orbital). Later EPR studies of frozen solutions of the radical allowed the anisotropic constants for the  $[\text{Mes}^*\text{PPMes}^*]^-$  radical anion to be determined and demonstrated that more than one species was present in solution.<sup>166</sup> The alkyl species also show hyperfine coupling to silicon,  $a(^{29}\text{Si}) = 5$  G. No satisfactory EPR spectrum of the diarsene radical anion was recorded. However, the EPR spectrum of the mixed phospharsene radical anion  $\text{DmtPASDmt}$  ( $\text{Dmt} = \text{C}_6\text{H}_2\text{-2,6-Mes}_2\text{-4-Me}$ ) showed hyperfine coupling to phosphorus [ $a(^{31}\text{P}) = 48$  G] and arsenic [ $a(^{75}\text{As}) = 23$  G], from which spin density distributions of 65% and 35% were estimated.<sup>167</sup>

The electrochemical and spectroscopic behavior of terphenyl-substituted diphosphenes has also been examined. These diphosphenes include  $\text{DmtPPDmt}$ ,  $\text{DxpPPDxp}$  [ $\text{Dxp} = 2,6\text{-di}(m\text{-xylyl})\text{phenyl}$ ], and  $\text{DmpPPDmp}$  ( $\text{Dmp} = \text{-C}_6\text{H}_2\text{-2,6-Mes}_2$ );<sup>168</sup> all displayed reversible reductions in THF at room temperature. Unexpectedly, they reduced at more negative potentials than  $\text{Mes}^*\text{PPMes}^*$  or  $(\text{Me}_3\text{Si})_3\text{CPPC}(\text{SiMe}_3)_3$ . For example, easier reduction might have been expected upon replacement of the  $\text{Bu}^t$  groups in  $\text{Mes}^*\text{PPMes}^*$  with two less electron-donating mesityl rings. The greater difficulty in reducing the terphenyl diphosphenes was attributed to the shorter and stronger P–P double bonds in these compounds, as a result of which the  $\pi^*$  levels lie at higher energies. Their solution EPR spectra at room temperature feature a signal that is centered at  $g = 2.008$ , with a coupling of 46 G to two equivalent <sup>31</sup>P nuclei, consistent with the presence of the unpaired electron in a  $\pi^*$ -orbital. Chemical reduction of the diphosphenes with sodium metal or sodium naphthalenide yielded the sodium salts  $\text{Na}[\text{ArPPAr}]$ , which show additional signals that were attributed to ion-pairing. No ion-pairing could be detected by EPR spectroscopy for the corresponding lithium, potassium, or magnesium salts.

Several radical derivatives of phosphorus–carbon multiply bonded compounds have also been generated at room temperature.<sup>149</sup> Electrochemical reduction of the phosphalkene  $(E)\text{-Mes}^*\text{P}=\text{C}(\text{H})\text{Ph}$  produces the radical anion  $[\text{Mes}^*\text{P}=\text{C}(\text{H})\text{Ph}]^-$ . The reduction is quasi-reversible ( $E_{1/2} = -1.98$  V vs SCE), and an EPR spectrum in THF solution at room temperature displayed a doublet pattern centered at  $g = 2.007$ , with further poorly resolved fine structure.<sup>169</sup> The main splitting is due to phosphorus and has a value of  $a(^{31}\text{P}) = 54.3$  G. The  $Z$  isomer gave the same results. The isotopically substituted isomers  $\text{Mes}^*\text{P}=\text{C}(\text{D})\text{C}_6\text{D}_5$ ,  $\text{Mes}^*\text{P}=\text{C}(\text{H})\text{C}_6\text{D}_5$ , and  $\text{Mes}^*\text{P}=\text{C}(\text{H})\text{Ph}$  allowed determination of the couplings for olefinic carbon [ $a(^{13}\text{C}) = 5.71$  G], alkene hydrogen

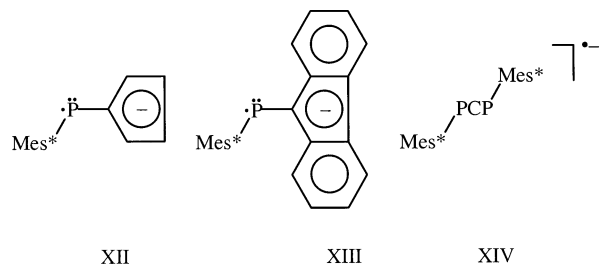
[ $a(^1\text{H}) = 4.64$  G], and phenyl hydrogens [2.5–3.93 G]. EPR studies of frozen solutions yielded the anisotropic  $^{31}\text{P}$  coupling constants, which were very similar to those of  $[\text{Mes}^*\text{PPMes}^*]^-$ . These showed that 0.4 of the spin density was in the phosphorus 3p-orbital. These results were in good agreement with ab initio calculations, which also predicted the location of the unpaired electron in a  $\pi^*$ -orbital and a spin density of 0.48 in each 3p-orbital in a hypothetical  $[\text{MePPMe}]^-$  radical.<sup>169</sup> The spin density on the unsaturated alkene carbon is considerably lower (ca. 0.15–0.18 in  $\text{C}_{2p}$ ). This was explained by delocalization of spin on the phenyl ring. Further studies on molecules containing two phosphaaalkene groups, as given by the compounds



as well as phosphaaalkenes linked by biphenyl or furan groups were conducted.<sup>170</sup> The presence of a second phosphaaalkene group in the molecules decreased the absolute value of the reduction potential. Both the EPR spectra and DFT calculations showed that the unpaired electron is in a  $\pi^*$ -orbital, and its delocalization is dependent on the relative position of the two phosphaaalkene groups and the type of bridging group. Small amounts of radical species were produced in addition to the major products. For the para species, equal coupling to two  $^{31}\text{P}$  nuclei, with  $a(^{31}\text{P}) = 43$  G, was observed. The ortho species displayed two couplings to  $^{31}\text{P}$  of 53.6 and 29.3 G, whereas the meta species showed equal hyperfine coupling to two phosphorus centers of 25.7 G. The different coupling constants in the ortho species are due to the *E,E* and *E,Z* isomers.

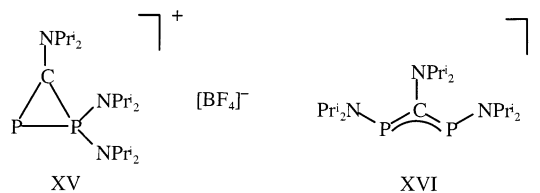
Other phosphorus radicals related to those derived from phosphaaalkenes include phosphafulvene<sup>171</sup> and diphosphaallene<sup>172</sup> radical anions, as indicated by **XII**–**XIV**. Cyclic voltammetry of DMF solutions of **XII** and **XIII** showed that they reduce at  $-1.200$  and  $1.349$  V. EPR solution spectroscopy of **XII** afforded a signal at  $g = 2.0039$ , with hyperfine splitting of 90 G due to coupling to  $^{31}\text{P}$ . The signal due to **XIII** was

observed at  $g = 2.0059$ , with  $a(^{31}\text{P}) = 78.9$  G. These parameters and ab initio calculations showed that the spin is located mainly in a phosphorus 3p-orbital. It may be noted that the splittings are considerably larger than those observed in the phosphaaalkenes [cf. 54.3 G in  $\text{Mes}^*\text{PC}(\text{H})\text{Ph}$ ], where there is significant spin delocalization.<sup>169</sup> The phosphafulvene couplings resemble those seen in the phosphinyl radicals.



Reduction of the phosphaaallene afforded the radical anion species **XIV**. The EPR spectrum of violet solutions of **XIV** in THF gave a signal that had hyperfine coupling to two equivalent  $^{31}\text{P}$  nuclei,  $a(^{31}\text{P}) = 76.8$  G (2P). A  $^{13}\text{C}$ -enriched anion displayed further coupling, with  $a(^{13}\text{C}) = 9.64$  G. The spectra are consistent with the unpaired electron being mainly localized on the two equivalent phosphorus atoms. Calculations at the semiempirical level showed that the trans-like isomer geometry is the more stable. Electrochemical work has also shown that the corresponding phosphaaallene cation  $[\text{Mes}^*\text{PCPMes}^*]^{+}$  could be generated.<sup>173</sup> At 300 K, the EPR spectrum persisted for 20 min after the electrolysis was terminated. It consisted of a 1:2:1 triplet pattern, indicating coupling to two equivalent phosphorus nuclei,  $a(^{31}\text{P}) = 31$  G (2P). Isotopic  $^{13}\text{C}$  enrichment at the central carbon site resulted in a new spectrum that displayed an additional coupling constant of ca. 31 G. No hyperfine couplings to hydrogens could be observed, suggesting that the  $\text{Mes}^*$  ring planes were perpendicular to the central PCP plane. Estimates of spin densities led to values of ca. 0.21 at each phosphorus and 0.51 in a p-orbital of the central carbon. Calculations on the model species  $[\text{HPCPH}]^{+}$  suggested that oxidation leads to the formation of two rotamers, one cis-like with a dihedral angle near  $45^\circ$ , and the other trans-like with a dihedral angle near  $135^\circ$ . There is a small energy difference that favors the cis-like isomer, but this may not be significant for the substituted species.

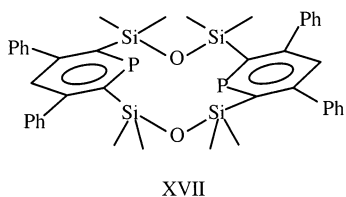
Preparative-scale electrolysis of the diphosphaacyclopropenium ion **XV** led to the deep red, air-sensitive **XVI**, which can also be generated by adding lithium



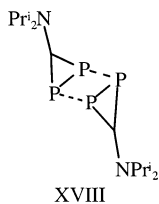
metal to a THF solution of **XV**.<sup>174</sup> It also proved possible to isolate the stable **XVI** as red crystals, although these were unsuitable for X-ray diffraction. The EPR signal of a THF solution of **XVI** displayed

a five-line pattern with an intensity ratio 1:3:4:3:1 due to coupling to two equivalent phosphorus and one nitrogen nucleus, with  $a(^{31}\text{P}) = 9.4$  G (2P) and  $a(^{14}\text{N}, I = 1) = 9.9$  G. The broadness of the signals suggested further hyperfine coupling, and simulation afforded further coupling to nitrogen, with  $a(\text{N}) = 1.5$  G (2N). Ab initio calculations showed that the symmetrical isomer of **XVI** is the only possible one that could have provided the symmetrical EPR spectrum.

Recent results<sup>175</sup> have disclosed the synthesis of a unique phosphorus radical species. Chemical and electrochemical reduction of the macrocycle **XVII** afforded a solution whose EPR spectral hyperfine tensors, in addition to DFT calculations, led to the conclusion that a one-electron  $\sigma$  P–P bond had been formed by overlap of phosphorus 3p-orbitals from the parallel rings. Reduction of **XVII** with sodium naphthalenide in THF at room temperature gave a purple solution. The EPR spectrum displayed a signal in a 1:2:1 pattern, with  $a(^{31}\text{P}) = 3.7$  G (2P). The small coupling constant arises from the fact that the principal values of the hyperfine tensor are of opposite sign and the fact that the P–P bond results from overlap of two 3p-orbitals. Unfortunately, it was not possible to grow crystals of **[XVII]**<sup>•−</sup> that were suitable for X-ray crystallography. DFT calculations on **XVII** models indicated a P–P distance of 2.763 Å (cf. P–P = 3.256 Å in the crystal structure; cf. ca. 2.2 Å for a single P–P bond). Further reduction afforded the dianion **[XVII]**<sup>2−</sup>, which was crystallized as its  $[\text{Na}(2.2.2)]^+$  salt. The two phosphinine moieties adopt a phosphacyclohexadienyl structure, linked by a P–P bond of 2.305(2) Å, significantly longer than the usual P–P single bond.



XVII



XVIII

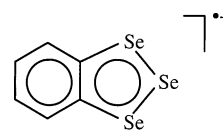
The structure of **XVIII** has parallels with that of **XVII**. It results from the weak dimerization  $[\text{P}^{\cdot-}\text{P} = 2.634(3)$  Å] of two  $\text{P}^{\cdot-}\text{C}_2\text{NPr}_2$  radicals. It was described as a singlet “diradical” with one-electron P–P bonds.<sup>176</sup> However, it does not dissociate in solution at room temperature, and no EPR signals were observed. The 1,3-diphosphacyclobutane-2,4-diyl  $\text{P}_2\text{C}_2$  four-membered ring system also may feature low-lying diradical states. In this case, the electron spins are located on the carbon rather than phosphorus atoms.<sup>177</sup>

The stable phosphorus radical  $\text{P}_3^{4-}$  (isoelectronic with  $\text{S}_3^-$ ) has been obtained as the blue-black salt  $\text{K}_4\text{P}_3$ .<sup>178</sup> Its characterization by X-ray crystallography was the first for a phosphorus radical. The  $\text{P}_3$  array has a bent structure, with a P–P bond length of 2.183 Å (consistent with multiple P–P bond character) and a P–P–P angle of 118.1°. Magnetic susceptibility measurements afforded a value of 1.6  $\mu_{\text{B}}$  (cf. 1.74  $\mu_{\text{B}}$  for one unpaired electron), although the temperature dependence of the paramagnetism does not follow

simple Curie–Weiss behavior. The EPR spectrum displayed a signal at  $g = 2.02$ , with a line width of 80, G with only ca. 20% of the expected intensity, which could be due to a quartet state or high electrical conductivity.

## V. Radicals of the Group 16 Elements Selenium and Tellurium

Radicals of selenium and tellurium have been less thoroughly studied than their sulfur counterparts. However, the area is of growing importance. One reason for this is the recognition that selenoenzymes play an important role in protection against free radical injury.<sup>179–181</sup> Another stems from the use of organoselenium compounds as precursors for radical reactions.<sup>182</sup> Some general aspects of the chemistry of selenium- and tellurium-centered radicals have been reviewed.<sup>179–183</sup> However, no persistent or stable derivatives were discussed. As with sulfur, the stable radicals of selenium or tellurium are, with rare exception, confined to delocalized species in which selenium or tellurium forms part of a carbon<sup>184–194</sup> or an element nitrogen, EN (E = Se or Te),<sup>195–207</sup> ring. Numerous paramagnetic compounds of these types are stable at or near room temperature. Examples from the former class of compounds include the deep violet benzo-1,2,3-triselenolium trifluorosulfonate salt **XIX**,<sup>189</sup> which produces gold-colored metallic crystals on removal of the solvent. The EPR spectrum in



XIX

acetonitrile showed a low-intensity singlet centered at  $g = 2.0758$ , with signal width at half-height of 26.5 G. When  $\text{CF}_3\text{COOH}$  was used as a solvent, the signal intensity increased considerably, indicating a solvent-dependent dissociation equilibrium. In the solid, the structure is dimerized through three long (ca. 3.15–3.25 Å) Se–Se interactions. Within the rings, the Se–Se distances are in the range 2.276(5)–2.298(5) Å (cf. 2.35 Å for a Se–Se single bond), indicating significant multiple character. There are also longer Se–Se interactions between the monomers. EPR studies on the 2,5-diphenylchalcophenes (chalcogen = O, S, Se, or Te), showed a coupling of 13.5 G between the unpaired electron and the <sup>125</sup>Te ( $I = 1/2$ , 7%) nucleus for the tellurophene derivative, demonstrating the presence of spin density at tellurium.

Cyclic paramagnetic species in which the ring consists of selenium and nitrogen were developed later than their sulfur counterparts. The first example<sup>195,196</sup> was obtained during the synthesis of  $(\text{SeNSeNSe}^-)_2(\text{AsF}_6)_2$ , which can dissociate to the  $7\pi$  radical  $[\text{SeNSeNSe}]^{\cdot+}$  in solution. In the solid, it dimerizes to the dication, which crystallizes as the  $(\text{AsF}_6)_2^{2+}$  salt with structures similar to those of the sulfur analogue<sup>197</sup> or the mixed species  $[\text{SeNSN}$



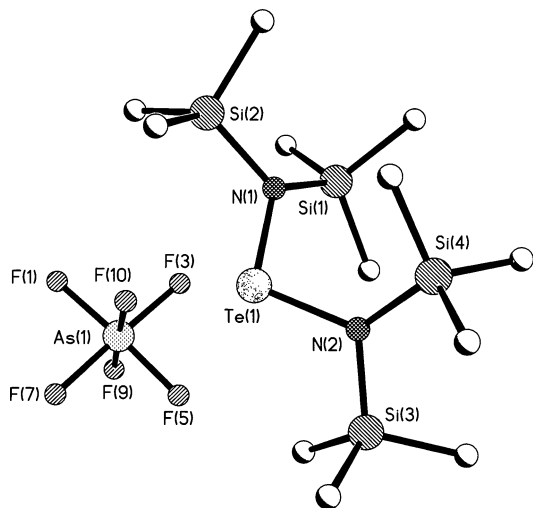
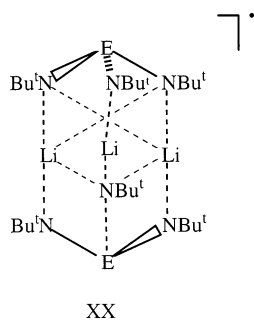


**Figure 14.** Schematic drawing of the structure of  $[\text{Te}\{\text{N}(\text{SiMe}_3)_2\}_2][\text{AsF}_6]^+$ .<sup>203</sup>

$\text{eNSe}^{\bullet+}$ )<sub>2</sub><sup>198</sup> and  $(\text{SeNSNS}^{\bullet+})_2$ .<sup>199</sup> Coupling to <sup>77</sup>Se ( $I = -1/2$ , 7.6%) was observed in the EPR spectrum at low temperatures. A number of other cyclic SeN species have also been characterized.<sup>197–202</sup>

Outside these two cyclic radical classes, the number of stable acyclic selenium or tellurium species is small. The most important is the stable radical cation  $[\text{Te}\{\text{N}(\text{SiMe}_3)_2\}_2]^+$ , which was obtained by oxidation of  $\text{Te}\{\text{N}(\text{SiMe}_3)_2\}_2$  with  $\text{AgAsF}_6$  and crystallized as its  $[\text{AsF}_6]^-$  salt.<sup>203</sup> It is the only structurally characterized heavier chalcogen radical species in which the spin is essentially un-delocalized. This was deduced from the EPR spectrum, which displayed a broad peak ( $\Delta w_{1/2} \approx 15$  G) in  $\text{CDCl}_3$  at room temperature, indicating a small spin density on the nitrogens. Thus, the unpaired electron is localized in a p-orbital on the chalcogen.  $[\text{Te}\{\text{N}(\text{SiMe}_3)_2\}_2]^+$  is analogous to the isovalent, neutral group 15 species  $:\text{E}\{\text{N}(\text{SiMe}_3)_2\}_2$  discussed earlier. The structure (Figure 14) showed interaction with its nearest  $[\text{AsF}_6]^-$  neighbors. The TeN distances, 1.964(4) and 1.968(4) Å, are shorter than the 2.053(2) and 2.045(2) Å Te–N bond lengths in  $\text{Te}\{\text{N}(\text{SiMe}_3)_2\}_2$ ,<sup>204</sup> consistent with the higher Te<sup>3+</sup> oxidation state in the radical cation.

Another radical in which an unpaired electron is located primarily on heavier chalcogens is  $\{\text{Li}_3[\text{E}(\text{NBu}^t)_3]_2\}^{\bullet}$  (E = S or Se).<sup>194,205,206</sup> The EPR spectrum of the sulfur compound displayed a signal at 2.0039,<sup>199</sup> with hyperfine coupling to both nitrogen [ $a(^{14}\text{N}) = 8^{206}$  or 5.69 G<sup>207</sup>] and lithium [ $a(^7\text{Li}, I = 3/2) = 0.8174$  or 0.82 G<sup>201</sup>], indicating the formation of a cage in which three lithiums bridge the nitrogens,



XX

as in **XX**. The parameters for the selenium derivative are  $g = 2.00652$ ,  $a(^{14}\text{N}) = 5.41$  G, and  $a(^7\text{Li}) = 0.79$  G. However, over a period of ca. 1 day, the seven-line pattern due to coupling to the three nitrogens is replaced by a 1:2:3:2:1 five-line pattern [ $a(^{14}\text{N}) = 13.4$  G] and later by a 1:1:1 three-line spectrum [ $a(^{14}\text{N}) = 15.4$  G and  $a(^{77}\text{Se}) = 4.3$  G], neither of which displays coupling to lithium. These spectra were assigned to the radical anions  $\text{SeO}(\text{NBu}^t)_2^{\bullet-}$  and  $\text{SeO}_2(\text{NBu}^t)^{\bullet-}$ . Similar work on the sulfur analogue gave corresponding sulfur–oxygen species.

## VI. Conclusions and Outlook

The results described in this review show that a wide range of radicals in which the unpaired electron is located primarily on a main-group element other than C, N, O, or S can be generated as persistent species. Furthermore, a growing number of these can be isolated in the solid state as stable compounds within the criteria given in ref 5. At present, the crystal structures of approximately two dozen stable or isolable radicals have been determined. Most of the crystal structures have been published within the last 10 years. A notable feature of the recent work has been the extension of the persistent or stable radical domain to the heavier group 13 elements Al, Ga, or In. In most cases, stabilization has been achieved with use of sterically encumbering ligands and/or delocalization.

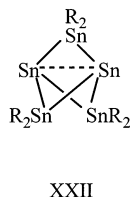
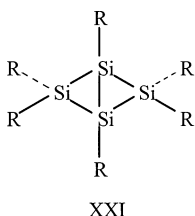
EPR spectroscopy has been the most important investigative tool in the study of all main-group radicals. Whereas  $g$ -factors do not deviate greatly from the free electron values, the observed hyperfine couplings, either to the main-group element itself or to its substituent atoms, have provided key information on the structures, bonding, hybridization (or lack thereof), and more rarely the reactivity of such radicals.

The synthesis of many of the radicals covered in this review has been inspired by analogies with their organic, i.e., carbon, nitrogen, or oxygen, counterparts. For example, the boron radicals  $[\text{BR}_3]^{\bullet-}$  and  $[\text{R}_2\text{BRR}_2]^{\bullet-}$ , and the aluminum and gallium radicals  $[\text{R}_2\text{MMR}_2]^{\bullet-}$  (M = Al or Ga) have a close electronic resemblance to the Gomberg radical  $[\text{CPh}_3]^{\bullet}$  or the cationic olefin radical  $[\text{R}_2\text{CCR}_2]^{\bullet+}$ . A similar analogy can be made for the heavier tetrel radicals  $[\text{MR}_3]^{\bullet}$  (M = Si–Sn) and the phosphalkene radical anions  $[\text{RP}=\text{CR}_2]^{\bullet-}$ . Nonetheless, many of the radicals have no organic counterparts. The group 13 cluster radicals  $[\text{B}_9\text{X}_9]^{\bullet-}$ ,  $[\text{B}_9\text{X}_9]^{\bullet-}$ ,<sup>62–67</sup>  $[\text{B}_{12}\text{Me}_{12}]^{\bullet-}$ ,<sup>70</sup>  $\cdot\text{CB}_{11}\text{Me}_{12}$ ,<sup>68</sup>  $[\text{Al}_6\text{Bu}_6]^{\bullet-}$ ,<sup>96</sup>  $[\text{Al}_{77}\{\text{N}(\text{SiMe}_3)_2\}_2]^{2\bullet-}$ ,<sup>101</sup> and  $[\text{M}_4\text{R}_4]^{\bullet-}$  (M = Ga or In; R = C(SiMe<sub>3</sub>)<sub>3</sub>)<sup>97</sup> have no “organic” analogues. Similarly, the group 14 polyhedra  $\text{M}_9^{3-}$  (M = Ge, Sn or Pb) have no carbon analogues.<sup>135–141</sup> Also, no persistent analogues of the radicals  $\text{R}^*\text{MMR}_2^*$  (M = Al or Ga;  $\text{R}^* = -\text{SiBu}_3$ ) are known in boron or carbon chemistry.<sup>103–105</sup>

Computational work on radical derivatives of the heavier main-group elements is currently not as extensive as it is in other areas of main-group chemistry, e.g., in multiply bonded compounds. However, this is changing rapidly. For example, computational data have afforded useful insights into the

M–M bonding in boron radical clusters<sup>69</sup> and group 13 radicals [RMMR<sub>2</sub>]<sup>•−</sup> (M = B, Al, or Ga; R = H or Ph),<sup>90,92</sup> and DFT calculations have provided structural parameters for R<sup>•</sup>AlAIR<sub>2</sub><sup>•</sup> (R = SiBu<sub>t</sub>).<sup>104</sup> Similarly, computational work has played a significant role in understanding the dissociation of the species R<sub>2</sub>EER<sub>2</sub> [E = P or As; R = CH(SiMe<sub>3</sub>)<sub>2</sub>], where it was shown that conformational changes within the bulky ligand CH(SiMe<sub>3</sub>)<sub>2</sub>, as well as interactions between the four ligands on the E–E unit, enable sufficient strain energy to be stored to effect E–E bond cleavage to the monomers: E{CH(SiMe<sub>3</sub>)<sub>2</sub>}<sub>2</sub> when the crystals are dissolved in hydrocarbon solvents.<sup>156</sup> DFT calculations on the radical Mes<sup>•</sup>-(Me)PPMes<sup>•</sup> have afforded parameters that were in excellent agreement with those determined experimentally.

The prediction of future developments in this field (as in any other) has inherent uncertainties. It seems reasonable to expect that numerous other examples from the persistent or stable radical classes already known will be synthesized. It is probable that the extensive range of radical species with multiple bonding to phosphorus can be extended to multiply bonded group 14 element species, where such radicals are currently rare. With greater difficulty, perhaps, it may be possible to extend radical domain to the group 2 elements, where persistent radical species of any kind are unknown. Developments in the area of stable diradicals may also be anticipated. Model species for the reported singlet diradical examples **VIII** and **XVIII** show that the electrons display significant coupling. For example, the triplet state of **VIII** lies over 17 kcal mol<sup>−1</sup> above the singlet state, suggesting that some bonding (possibly worth ca. 8–9 kcal mol<sup>−1</sup>) exists between the borons.<sup>71</sup> It can be argued that the bonding in several other main-group compounds bears a resemblance to that in **VIII**. For example, the diamagnetic tetrasiladicyclobutane **XXI**<sup>207</sup> and the pentastanna[1.1.1]propellane cluster **XXII**<sup>133</sup> display long transannular interelement dis-



tances that could be interpreted in terms of incipient biradical character. It is likely that the extent of interaction between the electrons in such compounds can be controlled in a rational way through electronic and steric effects.

A feature of the recent radical work is that many of the radicals were generated fortuitously en route to other objectives. Examples include the synthesis of the dialuminum and gallium radicals [R<sub>2</sub>MMR<sub>2</sub>]<sup>•−</sup>,<sup>72–74</sup> the aluminum cluster radicals<sup>101,102</sup> and the radicals R<sup>•</sup>MMR<sub>2</sub><sup>•</sup> (M = Al or Ga; R = −SiBu<sub>t</sub>),<sup>103–105</sup> and the ditin radical (THF)<sub>3</sub>NaR<sup>•</sup>SnSnAr<sup>•</sup>,<sup>130b</sup> where the anticipated products were even-electron species. The future will see a greater focus on designed stable radicals.

## VII. Acknowledgment

The authors thank Drs. A. Richards, A. D. Phillips, M. Brynda, and S. Hino for useful discussions and technical help as well as the National Science Foundation and the donors of the Petroleum Research Fund for financial support.

## VIII. Note Added in Proof

A concise review, entitled “Odd-Electron Bonds and Biradicals in Main Group Chemistry”, that deals with species such as those in refs 71 and 175 has been published (Grützmaier, H.; Breher, F. *Angew. Chem., Int. Ed.* **2002**, *41*, 4006). In addition, the author’s attention has been drawn to the fact that the use of large ligands such as barrelenes and substituted barrelenes has permitted the generation of persistent phosphinyl radicals, for example :PH(barrelene), in a crystalline matrix of PH<sub>2</sub>(barrelene) by irradiation with X-rays. The radicals are sufficiently persistent to be studied at room temperature. Detailed EPR studies, combined with density matrix analysis and DFT calculations, have allowed the determination of the **g**, <sup>31</sup>P, and <sup>1</sup>H hyperfine tensors as well as the intramolecular radical motion. Although the half-lives of the radicals at room temperature were not specifically given, it is clear that they are sufficiently long for extensive EPR studies at this temperature. See: Brynda, M.; Berclaz, T.; Geoffroy, M.; Ramakrishnan, G. *J. Phys. Chem. A* **1998**, *102*, 8245. Brynda, M.; Berclaz, T.; Geoffroy, M. *Chem. Phys. Lett.* **2000**, *323*, 474. Brynda, M.; Dutan, C.; Berclaz, T.; Geoffroy, M. *Curr. Top. Biophys.* **2002**, *26*, 35.

## IX. Note Added after ASAP Posting

This article was released ASAP on 2/22/2003 with an error in the reference number in the Figure 14 caption. Reference 203 is correct. The correct version was posted 3/12/2003.

## X. References

- (1) This statement usually applies to classical transition metal complexes with  $\sigma$ -donor ligands, but not to 18-electron complexes of  $\sigma$ -donor/ $\pi$ -acceptor ligands. For the general classification of transition metal complexes, see: Elschenbroich, Ch.; Salzer, A. *Organometallics: A Concise Introduction*, 2nd ed.; VCH: New York, 1992; p 186.
- (2) Only ns- and np-orbitals are available in main-group elements, since it seems likely that d-orbitals play little or no valence role in their bonding.
- (3) Examples include two-coordinate Be(Bu)<sup>•</sup>,<sup>a</sup> Be{N(SiMe<sub>3</sub>)<sub>2</sub>}<sub>2</sub>,<sup>b</sup> and Be{N(SiMe<sub>3</sub>)<sub>2</sub>}C<sub>6</sub>H<sub>3</sub>-2,6-Mes<sub>2</sub><sup>c</sup> and the one-coordinate compounds MC<sub>6</sub>H<sub>3</sub>-2,6-Trip<sub>2</sub> (M = In,<sup>d</sup> Tl;<sup>e</sup> Trip = C<sub>6</sub>H<sub>2</sub>-2,4,6-Pr<sub>3</sub>). Both types formally involve two empty valence p-orbitals. (a) Almenningen, A.; Haaland, A.; Nilson, J. E. *Acta Chem. Scand.* **1968**, *22*, 972. (b) Clark, A. H.; Haaland, A. *Chem Commun.* **1969**, 912. (c) Niemeyer, M.; Power, P. P. *Inorg. Chem.* **1997**, *36*, 4688. (d) Haubrich, S. T.; Power, P. P. *J. Am. Chem. Soc.* **1998**, *120*, 2202. (e) Niemeyer, M.; Power, P. P. *Angew. Chem., Int. Ed.* **1998**, *37*, 1277.
- (4) *Radical Ions*; Kaiser, E. T., Kevan, L., Eds.; Wiley: New York, 1968.
- (5) The terms “persistent” and “stable” have been applied to long-lived radicals. A persistent radical has a *relatively long lifetime* under the conditions it is generated, whereas a stable radical is inherently stable as an isolated species and shows no sign of decomposition under an inert atmosphere at room temperature. In this review, the use of the description “stable” will be confined to radicals that can be *isolated* under ambient conditions and can be stored without decomposition, either indefinitely or for long periods, at room temperature in the absence of air or

- moisture. Thus, the Gomborg radical,  $\cdot\text{CPh}_3$ ,<sup>9</sup> has been often described<sup>a,b</sup> as a stable radical, but it exists in equilibrium with its head-to-tail dimer in solution and is also dimerized as a solid. Similarly, the phosphinyl radical  $\cdot\text{P}\{\text{CH}(\text{SiMe}_3)_2\}_2$  (see later refs 25, 151, 155, and 156), which has a half-life of ca. 1 year in solution at room temperature, associates to form a weakly P–P bonded dimer in the crystal phase. Thus,  $\cdot\text{CPh}_3$  and  $\cdot\text{P}\{\text{CH}(\text{SiMe}_3)_2\}_2$  are persistent rather than stable radicals. In contrast, the boron radical  $[\text{Li}(12\text{-crown-}4)_2][\text{BMe}_3]$  is isolable as crystals (ref 43) at room temperature, where it is indefinitely stable in the absence of air and moisture. As a result,  $[\text{BMe}_3]^\cdot$  can be described as a stable radical. What constitutes a “relatively long lifetime” in the context of the description “persistent”? One definition is that it is sufficient time to allow the radical to be prepared in solution or in the solid state at room temperature under an inert atmosphere and to allow it to be spectroscopically and chemically characterized with conventional techniques.<sup>b</sup> These restrictions require a half-life of the order of minutes. However, as will be seen, several of the new main-group radicals have half-lives of at least several months or are indefinitely stable under such conditions. It seems probable that some of these persistent radicals will be isolated as stable crystalline species in the future. (a) Smith, M. B.; March, J. *March's Advanced Organic Chemistry: Reactions, Mechanisms and Structure*; Wiley: New York, 2001; p 238. (b) Forrester, A. R.; Hay, J. M.; Thomson, R. H. *Organic Chemistry of Stable Free Radicals*; Academic Press: London, 1968; p 1.
- (6) Frey, E. *Ann. Chim. Phys.* **1845**, 15, 459.
  - (7) Würster, C.; Sendtner, R. *Ber. Dtsch. Chem. Ges.* **1879**, 12, 1803.
  - (8) Beckmann, E.; Paul, T. *Ann. Chem.* **1891**, 266, 1.
  - (9) Gomborg, M. *J. Am. Chem. Soc.* **1900**, 22, 757; *Ber. Dtsch. Chem. Ges.* **1900**, 33, 3150.
  - (10) Rückardt, C. *Top. Curr. Chem.* **1980**, 88, 1.
  - (11) Sabacky, M. J.; Johnson, C. S., Jr.; Smith, R. G.; Gutowsky, H. S.; Martin, J. C. *J. Am. Chem. Soc.* **1967**, 89, 2054.
  - (12) *S-centered Radicals*; Alfassi, Z. B., Ed.; Wiley: New York, 1999.
  - (13) Glass, R. S. *Top. Curr. Chem.* **1999**, 205, 1.
  - (14) Preston, K. F.; Sutcliffe, L. H. *Magn. Reson. Chem.* **1990**, 28, 189.
  - (15) Cordes, A. W.; Haddon, R. C.; Oakley, R. T. In *Chemistry of Inorganic Ring Systems*; Steudel, R., Ed.; Elsevier: Amsterdam, 1992.
  - (16) Awere, E. G.; Burford, N.; Mailer, C.; Passmore, J.; Schriver, M. J.; White, P. S.; Banister, A. J.; Oberhammer, H.; Sutcliffe, L. H. *Chem. Commun.* **1987**, 66.
  - (17) Cameron, T. S.; Haddon, R. C.; Mattar, S. M.; Parsons, S.; Passmore, J.; Ramirez, A. P. *Chem. Commun.* **1991**, 358.
  - (18) Cameron, T. S.; Haddon, R. C.; Mattar, S.; Parson, S.; Passmore, J.; Ramirez, A. P. *Inorg. Chem.* **1992**, 31, 2274.
  - (19) Banister, A. J.; Bricklebank, N.; Lavender, I.; Rawson, J. M.; Gregory, C. T.; Tanner, B. K.; Clegg, W.; Elsegood, M. R.; Palacio, F. *Angew. Chem., Int. Ed. Engl.* **1996**, 35, 2533.
  - (20) Brownridge, S.; Du, H.; Fairhurst, S. A.; Haddon, R. C.; Oberhammer, H.; Parson, S.; Passmore, J.; Schriver, M. J.; Sutcliffe, L. H.; Westwood, N. P. C. *J. Chem. Soc., Dalton Trans.* **2000**, 3365.
  - (21) McManus, G. D.; Rawson, J. M.; Feeder, N.; Palacio, F.; Oliete, P. *J. Mater. Chem.* **2000**, 10, 2001.
  - (22) *Free Radicals*; Kochi, J. K., Ed.; Wiley: New York, 1973.
  - (23) Atkins, P. W.; Symons, M. C. R. *The Structure of Inorganic Radicals*; Elsevier: Amsterdam, 1966.
  - (24) Davidson, P. J.; Hudson, A.; Lappert, M. F.; Lednor, P. W. *Chem. Commun.* **1973**, 829.
  - (25) Gynane, M. J. S.; Hudson, A.; Lappert, M. F.; Power, P. P.; Goldwhite, H. *Chem. Commun.* **1976**, 623.
  - (26) Lappert, M. F.; Lednor, P. W. *Adv. Organomet. Chem.* **1976**, 14, 345.
  - (27) Krause, E.; Polack, H. *Ber. Dtsch. Chem. Ges.* **1926**, 59, 777.
  - (28) Krause, E.; Polack, H. *Ber. Dtsch. Chem. Ges.* **1928**, 61, 271.
  - (29) Krause, E.; Nobbe, P. *Ber. Dtsch. Chem. Ges.* **1930**, 63, 634.
  - (30) Krause, E.; Nobbe, P. *Ber. Dtsch. Chem. Ges.* **1931**, 64, 634.
  - (31) Chu, T. *J. Am. Chem. Soc.* **1953**, 75, 1730.
  - (32) Leffler, J. E.; Watts, G. B.; Tanigaki, T.; Dolan, E.; Miller, D. S. *J. Am. Chem. Soc.* **1970**, 92, 6825.
  - (33) Eisch, J. J.; Dluzniewski, T.; Behrooz, M. *Heteroat. Chem.* **1993**, 4, 235.
  - (34) Lankamp, H.; Nauta, W. T.; MacLean, C. *Tetrahedron Lett.* **1968**, 249.
  - (35) Chu, T. L.; Weismann, T. J. *J. Am. Chem. Soc.* **1956**, 78, 23.
  - (36) Chu, T. L.; Weismann, T. J. *J. Am. Chem. Soc.* **1956**, 78, 3610.
  - (37) Moeller, C. W.; Wilmarth, W. K. *J. Am. Chem. Soc.* **1959**, 81, 2638.
  - (38) Leffler, J. E.; Doland, E.; Tanigaki, T. *J. Am. Chem. Soc.* **1965**, 87, 927.
  - (39) Weissman, S. I.; vanWilligen, H. *J. Am. Chem. Soc.* **1965**, 87, 2285.
  - (40) Griffin, R. G.; vanWilligen, H. *J. Chem. Phys.* **1972**, 57, 86.
  - (41) Karplus, M.; Frankel, G. K. *J. Chem. Phys.* **1962**, 35, 1312.
  - (42) Adam, F. C.; Weissman, S. J. *J. Am. Chem. Soc.* **1958**, 80, 2057.
  - (43) Olmstead, M. M.; Power, P. P. *J. Am. Chem. Soc.* **1986**, 108, 4235.
  - (44) Elschenbroich, C.; Kühlkamp, P.; Behrendt, A.; Harms, K. *Chem. Ber.* **1996**, 129, 859.
  - (45) Kaim, W.; Schulz, A. *Angew. Chem., Int. Ed. Engl.* **1984**, 23, 65.
  - (46) Rajca, A.; Rajca, S.; Desai, S. R. *Chem. Commun.* **1995**, 1958.
  - (47) Schulz, A.; Kaim, W. *Chem. Ber.* **1989**, 122, 1863.
  - (48) Kwan, R. J.; Harlan, J.; Norton, J. R. *Organometallics* **2001**, 20, 3818.
  - (49) Berndt, A.; Klusik, H.; Schlüter, K. *J. Organomet. Chem.* **1981**, 222, C25.
  - (50) Biffar, W.; Nöth, H.; Pommerening, H. *Angew. Chem., Int. Ed. Engl.* **1980**, 19, 56.
  - (51) Schlüter, K.; Berndt, A. *Angew. Chem., Int. Ed. Engl.* **1980**, 19, 57.
  - (52) Klusik, H.; Berndt, A. *J. Organomet. Chem.* **1982**, 232, C21.
  - (53) Diborane(4) radicals of the type  $[\text{Ar}_2\text{BBAr}_2]^\cdot$  had earlier been implicated in the reduction of  $\text{Ar}_3\text{B}$  species. See ref 32.
  - (54) Klusik, H.; Berndt, A. *Angew. Chem., Int. Ed. Engl.* **1981**, 20, 870.
  - (55) Klusik, H.; Berndt, A. *J. Organomet. Chem.* **1982**, 234, C11.
  - (56) Moezzi, A.; Olmstead, M. M.; Power, P. P. *J. Am. Chem. Soc.* **1992**, 114, 2715.
  - (57) Moezzi, A.; Bartlett, R. A.; Power, P. P. *Angew. Chem., Int. Ed. Engl.* **1992**, 31, 102.
  - (58) Power, P. P. *Inorg. Chim. Acta* **1992**, 198–200, 443.
  - (59) Grigsby, W. J.; Power, P. P. *Chem. Commun.* **1996**, 2235.
  - (60) Grigsby, W. J.; Power, P. P. *Chem. Eur. J.* **1997**, 3, 368.
  - (61) Hoefelmeyer, J. D.; Gabbai, F. P. *J. Am. Chem. Soc.* **2000**, 122, 9054.
  - (62) Lewis, J. S.; Kaczmarczyk, A. *J. Am. Chem. Soc.* **1966**, 88, 1068.
  - (63) (a) Wong, E. H.; Kabbani, R. M. *Inorg. Chem.* **1981**, 19, 451. (b) Binder, H.; Kellner, R.; Vaas, K.; Hein, M.; Baumann, F.; Wanner, M.; Winter, R.; Kaim, W.; Hönle, W.; Grin, Y.; Wedig, W.; Schultheiss, M.; Kramer, R. K.; von Schnering, H. G.; Groeger, O.; Engelhardt, G. *Z. Anorg. Allg. Chem.* **1999**, 625, 1059.
  - (64) (a) Heinrich, A.; Keller, H.-L.; Preetz, W. *Z. Naturforsch. B* **1990**, 45, 184. (b) Lorenzen, V.; Preetz, W. *Z. Naturforsch.* **1997**, 52, 565.
  - (65) Lorenzen, V.; Preetz, W.; Baumann, F.; Kaim, W. *Inorg. Chem.* **1998**, 37, 4011.
  - (66) Wanner, M.; Kaim, W.; Lorenzen, V.; Preetz, W. *Z. Naturforsch. B* **1999**, 54, 1103.
  - (67) Speiser, B.; Tittel, C.; Einholz, W.; Schäfer, R. *Dalton Trans.* **1999**, 1741.
  - (68) King, B. T.; Noll, B. C.; McKinley, A. J.; Michl, J. *J. Am. Chem. Soc.* **1996**, 118, 10902.
  - (69) McKee, M. L. *J. Am. Chem. Soc.* **1997**, 119, 4220. McKee, M. L.; Wang, Z.-X.; Schleyer, P. v. R. *J. Am. Chem. Soc.* **2000**, 122, 4781.
  - (70) Peymann, T.; Knobler, C. B.; Hawthorne, M. F. *Chem. Commun.* **1999**, 2039. Hawthorne, M. F.; Peymann, T. U.S. Patent 6,355,840.
  - (71) Scheschkewitz, D.; Amil, H.; Gornitzka, H.; Schoeller, W. W.; Bourissou, D.; Bertrand, G. *Science* **2002**, 295, 1880.
  - (72) (a) Knight, L. B.; Kerr, K.; Miller, P. K.; Arrington, C. A. *J. Phys. Chem.* **1995**, 99, 16842. (b) Tague, T.; Andrews, L. *J. Am. Chem. Soc.* **1994**, 116, 4970.
  - (73) Treboux, G.; Barthelat, J.-C. *J. Am. Chem. Soc.* **1993**, 115, 4870.
  - (74) (a) Pluta, C.; Porschke, K.-R.; Kruger, C.; Hildebrand, K. *Angew. Chem., Int. Ed. Engl.* **1993**, 32, 388. (b) He, X.; Bartlett, R. A.; Olmstead, M. M.; Ruhlandt-Senge, K.; Sturgeon, B. E.; Power, P. P. *Angew. Chem., Int. Ed. Engl.* **1993**, 32, 717. (c) Uhl, W.; Vester, A.; Kaim, W.; Poppe, J. *J. Organomet. Chem.* **1993**, 454, 9.
  - (75) Kaim, W. *J. Organomet. Chem.* **1981**, 215, 325.
  - (76) Kaim, W. *J. Organomet. Chem.* **1981**, 215, 337.
  - (77) Kaim, W. *Z. Naturforsch. B* **1981**, 36, 677.
  - (78) Kaim, W. *Z. Naturforsch. B* **1982**, 37, 783.
  - (79) Braddock-Wilking, J.; Leman, J. T.; Farrar, C. T.; Larsen, S. C.; Singel, D. J.; Barron, A. R. *J. Am. Chem. Soc.* **1995**, 117, 1736.
  - (80) Cloke, F. G. N.; Hanson, G. R.; Henderson, M. J.; Hitchcock, P. B.; Raston, C. L. *Chem. Commun.* **1989**, 1002.
  - (81) Henderson, M. J.; Kennard, C. H. L.; Raston, C. L.; Smith, G. *Chem. Commun.* **1990**, 1203.
  - (82) Cloke, F. G. N.; Dalby, C. I.; Henderson, M. J.; Hitchcock, P. B.; Kennard, C. H. L.; Lamb, R. N.; Raston, C. L. *Chem. Commun.* **1990**, 1394.
  - (83) (a) Kaim, W.; Matheis, W. *Chem. Commun.* **1991**, 597. (b) The  $\text{Ga}(\text{dbab})_2$  complex may also be synthesized by the reaction of  $\text{GaCp}^*$  and dbab: Pott, T.; Jutzl, P.; Neumann, B.; Stämmler, H.-G. *Organometallics* **2001**, 20, 1965. (c) Diazabutadiene complexes of indium have also been reported: Baker, R. J.; Farley, R. D.; Jones, C.; Kloth, M.; Murphy, D. M. *Chem. Commun.* **2002**, 1196.

- (84) Barron, A. R. In *Coordination Chemistry of Aluminum*; Robinson, G. H., Ed.; VCH: Weinheim, 1993; Chapter 4, p 151.
- (85) Uhl, W. *Z. Naturforsch. B* **1988**, *43*, 1113.
- (86) Uhl, W.; Layh, M.; Hildenbrand, T. *J. Organomet. Chem.* **1989**, *364*, 289.
- (87) Uhl, W.; Layh, M.; Hiller, W. *J. Organomet. Chem.* **1989**, *368*, 139.
- (88) Wehmschulte, R. J.; Ruhlandt-Senge, K.; Olmstead, M. M.; Hope, H.; Sturgeon, B. E.; Power, P. P. *Inorg. Chem.* **1993**, *32*, 2983.
- (89) Uhl, W.; Schütz, U.; Kaim, W.; Waldhör, E. *J. Organomet. Chem.* **1995**, *501*, 79.
- (90) Bridgeman, A. J.; Nielsen, N. A. *Inorg. Chim. Acta* **2000**, *303*, 107.
- (91) Brothers, P. J.; Power, P. P. *Adv. Organomet. Chem.* **1996**, *39*, 1.
- (92) Hamilton, E. L.; Pruis, J. G.; DeKock, R. L.; Jalkanen, K. J. *Main Group Met. Chem.* **1998**, *21*, 219.
- (93) Uhl, W.; Vester, A.; Fenske, D.; Baum, G. *J. Organomet. Chem.* **1994**, *464*, 23.
- (94) Uhl, W.; Gerding, R.; Vester, A. *J. Organomet. Chem.* **1996**, *513*, 165.
- (95) Wehmschulte, R. J.; Power, P. P. *Angew. Chem., Int. Ed.* **1998**, *37*, 3152.
- (96) Dohmeier, C.; Mocker, M.; Schnöckel, H.; Lötze, A.; Schneider, U.; Alrichs, R. *Angew. Chem., Int. Ed. Engl.* **1993**, *32*, 1428.
- (97) Haaland, A.; Martinsen, K.-G.; Volden, H. V.; Kaim, W.; Waldhör, E.; Uhl, W.; Schütz, U. *Organometallics* **1996**, *15*, 1146.
- (98) (a) Schnöckel, H.; Schnepf, A. *Adv. Organomet. Chem.* **2001**, *47*, 235. (b) Schnöckel, H.; Schnepf, A. *Angew. Chem., Int. Ed.* **2002**, *41*, 3532.
- (99) Schnöckel, H.; Köhnlein, H. *Polyhedron* **2002**, *21*, 489.
- (100) Lam, W. H.; Lin, Z. *Polyhedron* **2002**, *21*, 503.
- (101) Ecker, A.; Weckert, E.; Schnöckel, H. *Nature* **1997**, *387*, 379.
- (102) Purath, A.; Köppe, R.; Schnöckel, H. *Chem. Commun.* **1999**, 1933.
- (103) Wiberg, N.; Amelunxen, K.; Nöth, H.; Kaim, W.; Klein, A.; Scheiring, T. *Angew. Chem., Int. Ed. Engl.* **1997**, *36*, 1213.
- (104) Wiberg, N.; Blank, T.; Kaim, W.; Schwerderski, B.; Linti, G. *Eur. J. Chem.* **2000**, 1475.
- (105) Wiberg, N.; Blank, T.; Amelunxen, K.; Nöth, H.; Knizek, J.; Habereden, T.; Kaim, W.; Wanner, M. *Eur. J. Inorg. Chem.* **2001**, 1719.
- (106) Iley, J. In *The Chemistry of Organic Germanium, Tin and Lead Compounds*; Patai, S., Ed.; Wiley: Chichester, 1995; Chapter 5.
- (107) Cotton, J. D.; Cundy, C. S.; Harris, D. H.; Hudson, A.; Lappert, M. F. *Chem. Commun.* **1974**, 651.
- (108) Hudson, A.; Lappert, M. F.; Lednor, P. W. *Dalton Trans.* **1976**, 2369.
- (109) Buschhaus, H.-U.; Lehnig, M.; Neumann, W. P. *Chem. Commun.* **1977**, 129.
- (110) Lehnig, M.; Neumann, W. P.; Wallis, E. *J. Organomet. Chem.* **1987**, *333*, 17.
- (111) Sakurai, H.; Mochida, K.; Kira, M. *J. Organomet. Chem.* **1977**, *124*, 235.
- (112) Gynane, M. J. S.; Lappert, M. F.; Rivière, P.; Rivière-Baudet, M. *J. Organomet. Chem.* **1977**, *142*, C9.
- (113) Mochida, K. *Bull. Chem. Soc. Jpn.* **1984**, *57*, 796.
- (114) Gynane, M. J. S.; Lappert, M. F.; Riley, P. I.; Rivière, P.; Rivière-Baudet, M. *J. Organomet. Chem.* **1980**, *202*, 5.
- (115) Lehnig, M.; Buschhaus, H.-U.; Neumann, W. P.; Apoussidis, T. *Bull. Soc. Chim. Belg.* **1980**, *89*, 907.
- (116) Buschhaus, H.-U.; Neumann, W. P.; Apoussidis, T. *Leibigs Ann. Chem.* **1981**, 1190.
- (117) Lehnig, M.; Apoussidis, T.; Neumann, W. P. *Chem. Phys. Lett.* **1983**, *100*, 189.
- (118) El-Faragay, A. F.; Lehnig, M.; Neumann, W. P. *Chem. Ber.* **1982**, *115*, 2783.
- (119) Gynane, M. J. S.; Harris, D. H.; Lappert, M. F.; Power, P. P.; Rivière, P.; Rivière-Baudet, M. *Dalton Trans.* **1977**, 2004.
- (120) Bennett, S. W.; Eaborn, C.; Hudson, A.; Jackson, R. A.; Root, K. D. *J. Chem. Soc. A* **1970**, 348. Cooper, J.; Hudson, A.; Jackson, R. A. *Mol. Phys.* **1972**, *23*, 209. Chatgililoglu, C.; Rossini, S. *Bull. Soc. Chem. Fr.* **1988**, 298.
- (121) Kyushin, S.; Sakurai, H.; Betsuyaku, T.; Matsumoto, H. *Organometallics* **1997**, *16*, 5386.
- (122) Kyushin, S.; Sakurai, H.; Matsumoto, H. *Chem. Lett.* **1998**, 107.
- (123) Kira, M.; Obata, T.; Kon, I.; Hashimoto, H.; Ichinoke, M.; Sakurai, H.; Kyushin, S.; Matsumoto, H. *Chem. Lett.* **1998**, 1097.
- (124) Apeloig, Y.; Bravo-Zhivotovskii, D.; Yzefovich, M.; Bendikov, M.; Shames, A. I. *Appl. Magn. Reson.* **2000**, *18*, 425.
- (125) McKinley, A. J.; Kanatsu, T.; Wallraff, G. M.; Miller, R. D.; Sooriyakumaran, R.; Michl, J. *Organometallics* **1988**, *7*, 2567. McKinley, J. A.; Kanatsu, T.; Wallraff, G. M.; Thompson, D. P.; Miller, R. D.; Michl, J. *J. Am. Chem. Soc.* **1991**, *113*, 2003.
- (126) Sekiguchi, A.; Matsuno, T.; Ichinoke, M. *J. Am. Chem. Soc.* **2001**, *123*, 12436.
- (127) Sekiguchi, A.; Fukawa, T.; Nakamoto, M.; Lee, V. Y.; Ichinoke, M. *J. Am. Chem. Soc.* **2002**, *124*, 9865.
- (128) Olmstead, M. M.; Pu, L.; Simons, R. S.; Power, P. P. *Chem. Commun.* **1997**, 1595.
- (129) Eichler, B. E.; Power, P. P. *Angew. Chem., Int. Ed.* **2001**, *40*, 796.
- (130) (a) Olmstead, M. M.; Simons, R. S.; Power, P. P. *J. Am. Chem. Soc.* **1997**, *119*, 11705. (b) Pu, L.; Haubrich, S. T.; Power, P. P. *J. Organomet. Chem.* **1999**, *582*, 100.
- (131) Pu, L.; Senge, M. O.; Olmstead, M. M.; Power, P. P. *J. Am. Chem. Soc.* **1998**, *120*, 12682.
- (132) Twamley, B.; Sofield, C. D.; Olmstead, M. M.; Power, P. P. *J. Am. Chem. Soc.* **1999**, *121*, 3357.
- (133) Sita, L. R.; Kinoshita, I. *J. Am. Chem. Soc.* **1992**, *114*, 7024.
- (134) Egorov, M. P.; Nefedov, O. M.; Lin, T.-S.; Gaspar, P. P. *Organometallics* **1995**, *14*, 1539.
- (135) Weidenbruch, M.; Kramer, K.; Schäfer, A.; Blum, J. K. *Chem. Ber.* **1985**, *118*, 107.
- (136) Critchlow, S. C.; Corbett, J. D. *J. Am. Chem. Soc.* **1983**, *105*, 5715.
- (137) Fässler, T. F. *Coord. Chem. Rev.* **2001**, *215*, 347.
- (138) Belin, C.; Mercier, H.; Angilella, V. *New J. Chem.* **1991**, *15*, 931.
- (139) Fässler, T. F.; Hunziker, M. *Inorg. Chem.* **1994**, *33*, 5380.
- (140) Fässler, T. F.; Hunziker, M. *Z. Anorg. Allg. Chem.* **1996**, *622*, 837.
- (141) Schütz, U. *Inorg. Chem.* **1999**, *38*, 1866.
- (142) Fässler, T. F.; Hunziker, M.; Spahr, M. E.; Lueken, H.; Schilder, H. *Z. Anorg. Allg. Chem.* **2000**, *606*, 692.
- (143) Walling, C.; Pearson, M. S. *Top. Phosphorus Chem.* **1966**, *3*, 1.
- (144) Bentrude, W. G. In *The Chemistry of Organophosphorus Compounds*; Hartley, F. R., Ed.; Wiley: Chichester, 1990; Vol. 1, Chapter 14.
- (145) Schmidt, U.; Kabitzke, K.; Markau, K.; Müller, A. *Chem. Ber.* **1966**, *99*, 1497.
- (146) Kochi, J. K.; Krusic, P. J. *J. Am. Chem. Soc.* **1969**, *91*, 3944.
- (147) Roberts, B. P. *Adv. Free Radical Chem.* **1980**, *6*, 225.
- (148) Tordo, P. In *The Chemistry of Organophosphorus Compounds*; Hartley, F. R., Ed.; Wiley: Chichester, 1990; Vol. 1, Chapter 6.
- (149) Geoffroy, M. *Recent Res. Dev. Phys. Chem.* **1998**, *2*, 311.
- (150) Geoffroy, M.; Berclaz, T. In *The Chemistry of Organic Arsenic Antimony and Bismuth Compounds*; Patai, S., Ed.; Wiley: Chichester, 1994; Chapter 12.
- (151) Gynane, M. J. S.; Hudson, A.; Lappert, M. F.; Power, P. P.; Goldwhite, H. *Dalton Trans.* **1980**, 2428.
- (152) Cetinkaya, B.; Hudson, A.; Lappert, M. F.; Goldwhite, H. *Chem. Commun.* **1982**, 609.
- (153) Griller, D.; Roberts, B. P.; Davis, A. G.; Ingold, K. U. *J. Am. Chem. Soc.* **1974**, *96*, 554.
- (154) Geoffroy, M.; Ginet, L.; Lucken, E. A. C. *J. Chem. Phys.* **1976**, *65*, 729.
- (155) Hinchley, S. L.; Morrison, C. A.; Rankin, D. W. H.; Macdonald, C. L.; Wiacek, R. J.; Cowley, A. H.; Lappert, M. F.; Gundersen, G.; Clyburne, J. A. C.; Power, P. P. *Chem. Commun.* **2000**, 2045.
- (156) Hinchley, S. L.; Morrison, C. A.; Rankin, D. W. H.; Macdonald, C. L. B.; Wiacek, R. J.; Voigt, A. H.; Cowley, A. H.; Lappert, M. F.; Gundersen, G.; Clyburne, J. A. C.; Power, P. P. *J. Am. Chem. Soc.* **2001**, *123*, 9045.
- (157) Hitchcock, P. B.; Lappert, M. F.; Power, P. P.; Smith, S. J. *Chem. Commun.* **1984**, 1669.
- (158) Hitchcock, P. B.; Lappert, M. F.; Smith, S. J. *J. Organomet. Chem.* **1987**, *320*, C27.
- (159) Cattani-Lorente, M.; Geoffroy, M. *J. Chem. Phys.* **1989**, *91*, 1498.
- (160) Loss, S.; Widauer, C.; Grützmacher, H. *Angew. Chem., Int. Ed.* **1999**, *38*, 3329.
- (161) Loss, S.; Magistrato, A.; Cataldo, L.; Hoffmann, S.; Geoffroy, M.; Röthlisberger, U.; Grützmacher, H. *Angew. Chem., Int. Ed.* **2001**, *40*, 723.
- (162) Sasaki, S.; Murukami, F.; Yoshifuji, M. *Angew. Chem., Int. Ed.* **1999**, *38*, 340.
- (163) Roberts, B. P.; Singh, K. *Perkin Trans. 2* **1981**, 867.
- (164) Bard, A. J.; Cowley, A. H.; Kilduff, J. E.; Leland, J. K.; Norman, N. C.; Pakulski, M.; Heath, G. A. *Dalton Trans.* **1987**, 249.
- (165) Culcasi, M.; Gronchi, G.; Escudé, J.; Couret, C.; Pujol, L.; Tordo, P. *J. Am. Chem. Soc.* **1986**, *108*, 3130.
- (166) Geoffroy, M.; Cattani-Lorente, M. *J. Chem. Phys.* **1991**, *88*, 1159.
- (167) Tsujii, K.; Fujii, Y.; Sasaki, S.; Yoshifuji, M. *Chem. Lett.* **1997**, 855.
- (168) Shah, S.; Burdette, S. C.; Swavey, S.; Urbach, F. L.; Protasiewicz, J. D. *Organometallics* **1997**, *16*, 3395.
- (169) Geoffroy, M.; Jouaiti, A.; Terron, G.; Cattani-Lorente, M.; Ellinger, Y. *J. Phys. Chem.* **1992**, *96*, 8241.
- (170) Al Badri, A.; Jouaiti, A.; Geoffroy, M. *Magn. Reson. Chem.* **1999**, *37*, 735.
- (171) Al Badri, A.; Chentit, M.; Geoffroy, M.; Jouaiti, A. *Faraday Trans.* **1997**, *93*, 3631.
- (172) Sidorenkova, H.; Chentit, M.; Jouaiti, A.; Terron, G.; Geoffroy, M.; Ellinger, Y. *Perkin Trans. 2* **1998**, 71.
- (173) Chentit, M.; Sidorenkova, H.; Jouaiti, A.; Terron, G.; Geoffroy, M.; Ellinger, Y. *Perkin Trans. 2* **1997**, 921.
- (174) Canac, Y.; Baceiredo, A.; Schoeller, W. W.; Gignes, D.; Bertrand, G. *J. Am. Chem. Soc.* **1997**, *119*, 7579.

- (175) Cataldo, L.; Choua, S.; Berclaz, T.; Geoffroy, M.; Mézailles, N.; Ricard, L.; Mathey, F.; Le Floch, L. *J. Am. Chem. Soc.* **2001**, *123*, 6654.
- (176) Canac, Y.; Bourissou, D.; Baceiredo, A.; Gornitzka, H.; Schoeller, W. W.; Bertrand, G. *Science* **1998**, *279*, 2080.
- (177) Niecke, E.; Fuchs, A.; Baumeister, F.; Nieger, M.; Schoeller, W. *Angew. Chem., Int. Ed. Engl.* **1995**, *34*, 555. Niecke, E.; Fuchs, A.; Nieger, M. *Angew. Chem. Int. Ed.* **1999**, *38*, 3028. Niecke, E.; Fuchs, A.; Nieger, M.; Schmidt, O.; Schoeller, W. *Angew. Chem., Int. Ed.* **1999**, *38*, 3031.
- (178) von Schnering, H.-G.; Hartwig, M.; Hartwig, U.; Hönle, W. *Angew. Chem., Int. Ed. Engl.* **1989**, *28*, 56.
- (179) Richard, M. J.; Koukay, N.; Faver, A. *Med. Nutr.* **1987**, *23*, 291.
- (180) Jackson, M. J.; Edwards, R. H. T. *Curr. Top. Nutr. Dis.* **1988**, *18*, 431.
- (181) Burk, R. F. *Pharmacol. Ther.* **1990**, *45*, 383.
- (182) Renaud, D. *Top. Curr. Chem.* **2000**, *208*, 81.
- (183) Deryagina, E. N.; Voronkov, M. G. *Sulfur Rep.* **1995**, *17*, 89.
- (184) Chiu, M. F.; Gilbert, B. C. *J. Chem. Soc., Perkin Trans. 2* **1973**, 258.
- (185) Bock, H.; Brachler, G.; Dauplaise, D.; Meinwald, J. *Chem. Ber.* **1981**, *114*, 2622.
- (186) Jones, M. T.; Jansen, S.; Acampona, L. A.; Sandman, D. J. *J. Phys. Colloq.* **1983**, 1159.
- (187) Kato, R.; Kobayashi, H.; Kobayashi, A. *Physica B+C* **1986**, *143*, 304.
- (188) Davies, A. G.; Shiesser, C. H. *J. Organomet. Chem.* **1990**, *389*, 301.
- (189) Wolmershäuser, G.; Heckmann, G. *Angew. Chem., Int. Ed. Engl.* **1992**, *31*, 779.
- (190) Wolmershäuser, G.; Kaim, W.; Heckmann, A.; Lichtblau, A. *Z. Naturforsch. B* **1992**, *47*, 143.
- (191) Imakubo, T.; Okano, Y.; Sawa, H.; Kato, R. *Chem. Commun.* **1995**, 2493.
- (192) Okano, Y.; Yamamoto, K.; Imakubo, T.; Sawa, H.; Kato, R. *Synth. Met.* **1997**, *86*, 1829.
- (193) Gleiter, R.; Röckel, H.; Neugebauer, F. A. *J. Org. Chem.* **1996**, *61*, 1739.
- (194) Nakata, M.; Kobayashi, A.; Saito, T.; Kobayashi, H.; Takimiyu, K.; Otsubo, T.; Oguro, F. *Chem. Commun.* **1997**, 593.
- (195) Awere, E. G.; Passmore, J.; White, P. S.; Klapötke, T. *Chem. Commun.* **1989**, 1415.
- (196) Awere, E. G.; Passmore, J.; White, P. S. *Dalton Trans.* **1993**, 299.
- (197) Banister, A. J.; Clarke, H. G.; Rayment, I.; Shearer, H. M. M. *Inorg. Nucl. Chem. Lett.* **1974**, *10*, 647.
- (198) Gillespie, R. J.; Kent, J. P.; Sawyer, J. F. *Inorg. Chem.* **1981**, *20*, 4053.
- (199) Awere, E. G.; Brooks, W. V. F.; Passmore, J.; White, P. S.; Sun, X.; Cameron, T. S. *Dalton Trans.* **1993**, 2439.
- (200) Awere, E. G.; Passmore, J.; Preston, K. F.; Sutcliffe, L. H. *Can. J. Chem.* **1988**, *66*, 1776.
- (201) Boéré, R. T.; Larsen, K.; Fait, J.; Yip, J.; Moock, K. H. *Phosphorus, Sulfur, Silicon Relat. Elem.* **1992**, *65*, 143.
- (202) Rawson, J. M.; Banister, A. J.; May, I. *Magn. Reson. Chem.* **1994**, *32*, 487.
- (203) Björgvinsson, M.; Heinze, T.; Roesky, H. W.; Pauer, F.; Stalke, D.; Sheldrick, G. M. *Angew. Chem., Int. Ed. Engl.* **1991**, *30*, 1677.
- (204) Björgvinsson, M.; Roesky, H. W.; Pauer, F.; Stalke, D.; Sheldrick, G. M. *Inorg. Chem.* **1990**, *29*, 5140.
- (205) Fleischer, R.; Freitag, S.; Pauer, F.; Stalke, D. *Angew. Chem., Int. Ed. Engl.* **1996**, *35*, 204.
- (206) Fleischer, R.; Freitag, S.; Stalke, D. *Dalton Trans.* **1998**, 193.
- (207) Brask, J. K.; Chivers, T.; McGarvey, B.; Schalte, G.; Sung, R.; Boéré, R. T. *Inorg. Chem.* **1998**, *37*, 4633.
- (208) Masamune, S.; Kabe, Y.; Collins, S.; Williams, D. J.; Jones, R. *J. Am. Chem. Soc.* **1985**, *107*, 5552. Jones, R.; Williams, D. J.; Kabe, Y.; Masamune, S. *Angew. Chem., Int. Ed. Engl.* **1986**, *25*, 125. Schleyer, P. v. R.; Sax, A. F.; Kalcher, J.; Janaschek, R. *Angew. Chem., Int. Ed. Engl.* **1987**, *26*, 364.

CR020406P

